



Title	Robust and efficient quantum communication based on decoherence-free subspace
Author(s)	Kumagai, Hidetoshi
Citation	大阪大学, 2013, 博士論文
Version Type	VoR
URL	https://hdl.handle.net/11094/27509
rights	二次配布には著者本人による許諾が必要
Note	

Osaka University Knowledge Archive : OUKA

<https://ir.library.osaka-u.ac.jp/>

Osaka University

17 16325

**Robust and efficient quantum communication based on
decoherence-free subspace**

Hidetoshi Kumagai

MARCH 2013

Robust and efficient quantum communication based on decoherence-free subspace

A dissertation submitted to
THE GRADUATE SCHOOL OF ENGINEERING SCIENCE
OSAKA UNIVERSITY
in partial fulfillment of the requirements for the degree of
DOCTOR OF PHILOSOPHY IN SCIENCE

Presented by

Hidetoshi Kumagai

MARCH 2013

Abstract

Faithful distribution of photonic entangled states among distantly located parties is one of the important issues in the field of quantum communication. Embedding the quantum states into decoherence-free subspace (DFS) consisting of a number of photons is considered to be one of the promising schemes to achieve this task. So far several schemes have been proposed and experimentally demonstrated for quantum communication. The photon loss in the quantum channel, however, seriously degrades the transmission rate of quantum states. For example, when the transmittance of one photon through the channel is T and the number of photons to build the DFS is two, the transmission rate of a signal quantum state is proportional to T^2 .

Recently, in order to boost up the efficiency of the DFS, a new entanglement sharing protocol has proposed and experimentally demonstrated. The success probability of this scheme is proportional to T , in spite of a two-photon DFS. The key idea of this scheme is the use of an ancillary photon from a weak coherent light pulse counter-propagating through the channels to build the two photon DFS. This scheme is, however, robust against only a phase noise channel.

In this thesis, we propose an entanglement distribution scheme which is robust against not only a phase noise but also a general type of the channel noise and the transmission rate is proportional to T .

Acknowledgments

I would like to thank Prof. Nobuyuki Imoto for kindly accepting me to join his Laboratory. Through my research life, he provided me a terrific studying environment and gave me important advices for my research. Furthermore, he taken over preparing troublesome documents many times for me. I am so grateful to Prof. Masato Koashi. During the discussion I was surprised many times at his incisive insights. Also after leaving Osaka University, we gave me some significant advices. I would like to say thank you to Prof. Takashi Yamamoto. He also gave me important advices with respect to my research. Not only that but he kindly corrected my abstracts, a paper, and this thesis. Without his support, I would not finish my research.

Special thanks to Dr. Rikizo Ikuta and Toshiyuki Yamagata for their fruitful discussions. A lot of time was spent discussing with me. In some situation, it was continued until late at night. Now, it is a pleasant memory. I would like to appreciate Yoritoshi Adachi and Koji Azuma. They taught me when I was in trouble and dealt with my questions.

I appreciate all member of Imoto Lab. for supporting me in many situations and for their friendship. I am grateful to Aya Bouno for supporting my activities. I also appreciate the member of my futsal team. Thanks to them, I had a great time in Osaka. I would like to thank Global COE Program for financial support.

Finally, I would like to thank Masafumi Kumagai , Kayo Kumagai, and Reina Kumagai for encouragement. Thanks to their warm support, I could finish this thesis.

Contents

1	Introduction	1
2	Polarization-state transformation in an optical fiber	6
2.1	Polarization-state transformation in the lossless media	6
2.1.1	Definitions	6
2.1.2	Polarization-state transformation in a lossless birefringent element	10
2.1.3	Examples of the polarization-state transformation 1	11
2.2	Polarization-state transformation in a lossless birefringent elements for the backward-propagating photon	13
2.2.1	The matrix of the birefringent element for the backward-propagating photon	13
2.2.2	Examples of the polarization-state transformation 2	14
2.2.3	The matrix of the optical fiber	18
2.3	Backward propagation and the time-reversal symmetry	19
2.3.1	Antiunitary operator	19
2.3.2	Time-reversal operator	21
2.3.3	Relation between backward propagation and the time-reversal symmetry	24
2.4	Polarization-state transformation in reciprocal media	26
2.5	The universal compensator	28
2.5.1	The universal compensator	29
2.6	discussion	32
2.7	Summary	34
3	Quantum communication based on the DFS	36
3.1	Introduction to the DFS based quantum communication	36
3.2	Single-qubit distribution protocol over collective phase noise	37
3.3	Single-qubit distribution protocol over general collective noise	41
3.4	4-qubit DFS protocol	42

4	Entanglement distribution protocol with counter-propagating photons	45
4.1	Equivalent operation on entangled states	45
4.2	Counter-propagating protocol	47
4.3	Boosting up the efficiency using WCP	47
4.4	Discussion	48
4.5	Summary	49
5	Entanglement distribution protocol over general collective noise with counter-propagating photons	51
5.1	Working principle of the proposed protocol	51
5.2	Time-bin protocol	54
5.3	Discussions	57
5.3.1	Discussion1- Robustness against the unbalance of the transmission efficiency	57
5.3.2	Discussion2- Interpretation	57
5.3.3	Discussion3-Application range of our protocol	58
5.4	Summary	61
6	Conclusion	62
A	Appendix for Chap. 2	64
A.1	Bell states	64
A.2	The expression of Eq. (2.17) with arbitrary coordinate systems	64

Chapter 1

Introduction

Quantum mechanical world offers strange behavior, which is not easy to understand from the classical viewpoint. The cat which is in the superposition state of the living and death was introduced by Schrödinger to show the strangeness of the quantum mechanics [1]. The strange nature of quantum world even bothered a famous physical scientist A. Einstein and his colleagues and they criticized the quantum mechanics using an example of the specific quantum state, which is called EPR state or entangled state [2]. About 30 years later from the EPR paper, an interesting inequality which shows the borderline between the classical world and the quantum world was proposed by J. S. Bell [3]. This inequality, which is called Bell's inequality, is a simple one which makes classically plausible assumptions - locality and reality. A generalized inequality of Bell's inequality, which is called CHSH inequality, was also proposed by J. F. Clauser, M. A. Horne, A. Shimony, and R. A. Holt [4]. The violation of Bell's inequality is presented using entangled state which is used to show the contradiction of the quantum mechanics. Ironically, in fact, the violation of Bell's inequality was confirmed experimentally by A. Aspect *et al* [5]. This means that, whether we like it or not, all the things that happens in the real world are not explained by classical language only.

Quantum mechanics has brought out many facts what happen in the world. One of the example of the curious but incomprehensible phenomenon which was explained by the quantum mechanics is the double-slit experiment. In this experiment, in spite of the emission of the single particle, the interference pattern appears if the trials are repeated. To understand the result of this experiment, we have to accept the fact that such a particle cannot be treated just as a usual classical particle. We have to accept the dual nature - wave nature and particulate behavior. Other than that, for example, the discrete energy levels of the hydrogen atom is explained by using the quantum mechanics. As seen above, quantum mechanics has successfully explained the phenomena of nature.

Quantum mechanics has mainly developed in the field of elementary particle physics, cosmology,

and condensed matter physics. Recently, a new attempt to understand the information science by physics has been done. This area is, in a broad sense, called quantum information [6]. A basic idea of the quantum computing machine (quantum Turing machine), which is one of the biggest topic of quantum information, was first proposed by D. Deutsch [7]. In his idea, the bits is not treated as a classical bits which have the fixed values, but as the superposition of the bits. This quantum version of bit is called qubit. The basic idea of the quantum Turing machine is that during the calculation, the parallel computation by use of the superposition states of the bits is performed. He showed that arbitrary quantum circuits are simulated by this quantum Turing machine. At that time, however, quantum Turing machine was just a toy *gedanken*.

In 1994, P. W. Shor proposed a sensational quantum algorithm which can factor a big number in a polynomial time [8]. This implies that if the quantum computing machine is realized, the public key cryptosystem, which is now used all over the world, would break down. Since then, quantum information has got a lot of attention. Other than that, a useful quantum data search algorithm was proposed by Grover [9]. They showed the potentiality of quantum computing machine.

Nowadays, quantum information became an established area of physics and has a wide variety of research topics. Among them, quantum communication is one of the important topic. A big challenge of the quantum communication is to diffuse the use of quantum networks around the world as well as the present networks [10]. The first step of quantum networks is to distribute entangled qubits between two users and then expand to the multi-party entangled system such as W states [11, 12, 13, 14] or GHZ [15, 16] states. A short-range to a long-range entangled system is also an important element. This can be realized using well known quantum repeater protocol [17, 18, 19, 20, 21], which repeats the entanglement generation and entanglement swapping [22] using repeaters with quantum memories. In order to implement quantum information processing such as quantum teleportation [23], entanglement based quantum key distribution (QKD) [24, 25, 26] and quantum computation [27, 28] between two-parity Alice (sender of the signal state) and Bob (receiver of the signal state), they have to share entangled pair in advance. Since they cannot share entangled pair by using only local operations and classical communications (LOCC), Alice has to prepare it and send a half of entangled pair. In the entanglement sharing, the photons are best suited candidate of the qubits.

The signal photon is sent from Alice to Bob through an optical fiber, however, there are annoying obstacles during the transmission of the photon. The quantum state is naive and fragile, and it is vulnerable to the channel noise. This cause the breaking of the initial entangled state which Alice prepared, and this makes quantum information processing hard to implement. The typical kind of the channel noises are the phase noise and the polarization rotation which come from the birefringent effect of the channel. The difference of the refractive indices depending on the crystal axes cause the birefringence. Protecting the quantum state from the channel noise is important issues. Roughly

speaking, there are two effective ways to circumvent the degradation of the quantum states. One possible way is quantum error correction (QEC) and the other is to use the decoherence-free subspace (DFS).

The first candidate, QEC, is to encode the qubits into error correcting codes, which are well designed error correctable codes, e.g., CSS code employing 7 qubits. Alice encodes qubits into this code and sends all of them. After receiving these qubits, Bob implements the error correction and decodes back to the initial state. In this case, however, the distribution efficiency is $O(T^7)$, since seven qubits are required to construct CSS code, and all the qubits has to be delivered. Here T represents the transmittance of the channel. This idea is unsuited to distribution of the quantum state.

The second promising candidate is the use of the *noiseless subspace*, called decoherence-free subspace (DFS) [29, 30]. The DFS is a part of the Hilbert space and qubits are encoded within the space spanned by this subspace. Compared to the former scheme, less qubits are needed and the distribution efficiency is high. Another advantage of this scheme is the unnecessary of the active controls. Alice just sends the signal photon with the signal photon. The ancillary photon helps to construct the such a noiseless subspace by expanding Hilbert space. After receiving the photons, all Bob has to do is to decode back to the initial state. DFS is a powerful tool and this idea is used not only in the quantum communication but also in many situations [31, 32, 33, 34, 35].

This thesis is mainly focused on entanglement distribution schemes based on DFS. Until now, in quantum communication, many efforts have been made theoretically and experimentally [36, 37, 38, 39, 40, 41, 42, 43, 44, 45, 46]. With respect to the single qubit distribution and entanglement distribution, the comparison of the robustness and the efficiency of the protocols are shown in Table 1. As shown, our protocol shows the best performance.

The organization of this thesis is as follows:

Chapter 2: Polarization state transformation in an optical fiber

In this chapter, we examine the polarization-state transformation in birefringent media using Jones method. The birefringent media are the model of the optical fiber that is widely used as the communication channel. More importantly, we give a useful relation of the birefringent media for the forward-propagating and backward-propagating photon. This relation is used in our newly proposed entanglement distribution protocol.

Chapter 3: Quantum communication based on the DFS

We review faithful single qubit distribution among the distantly separated parties. This is a significant task for the quantum communication and still central theme in this area. In this chapter, we use the DFS which is useful noise-suppressing scheme against the fluctuations of the transmission

Scheme	Phase noise	General noise	Efficiency
M. Bourennane <i>et. al.</i>	○	○	T^4
T. Yamamoto <i>et. al.</i>	○	○	T^2
R. Ikuta <i>et. al.</i>	○	×	T
<i>This thesis</i>	○	○	T

Table 1.1: Comparison of the robustness and the efficiency between previous schemes and our scheme.

channel. We show that the signal photon with an ancillary photon enables us to distribute an arbitrary single qubit state under the collective phase noise. Then we show that by using additional transmission lines, it becomes possible to overcome a general type of the channel noise. This scheme is easily generalize to entanglement distribution scheme.

Chapter 4: Entanglement distribution protocol with counter-propagating photons

In the conventional protocols, all the photons forming DFS, i.e., the signal and the ancillary photons have to delivered to the receiver's side. This restriction fatally decreases the transmission rate of the scheme. The success probability of the DFS schemes which are introduced in chapter 3 is proportional to T^2 . This means that when $T = 0.01$, the success probability becomes 10^{-4} .

In this chapter, we introduce an efficient entanglement distribution protocol which can achieve the success probability to be proportional to T . An essential idea is to use a weak coherent light pulse as an ancillary photon from the receiver of the signal photon to the sender. This idea shed light on a new entanglement distribution scheme and is taken in the scheme proposed in chapter 5.

Chapter 5: Entanglement distribution protocol over general collective noise with counter-propagating photons

We have introduced an efficient entanglement distribution scheme in chapter 4. The robustness in this scheme is assumed only the phase noise. In general, however, the polarization rotations exist

during the transmission.

In this chapter, we propose a new entanglement distribution protocol which is robust against not only a phase noise but also a general noise. This scheme is also efficient one that can achieve the success probability to be proportional to T . At the end of this chapter, we discuss the application range of the counter-propagating DFS protocols. Is it possible to apply the counter-propagating DFS schemes to all kind of the transmission channel? We answer this question.

Chapter 2

Polarization-state transformation in an optical fiber

2.1 Polarization-state transformation in the lossless media

2.1.1 Definitions

In order to analyze the polarization-state transformation in an optical fiber, we use Jones calculation method, which enables us to calculate the output state of the photon if the input state and the transformation matrix of the optical fiber are given. The first thing which we have to do is to clarify the definition of the polarization of the photons for which avoid the unwanted confusion of the polarization state during the transmission of the fiber. First we introduce the coordinate systems used in this paper to describe the polarization states for forward-propagation (Alice to Bob) and backward-propagating (Bob to Alice) photons. Our definitions of the polarization-state used in this paper are as follows:

- We assign two right-handed coordinate systems xyz and $x'y'z'$, which are used for forward- and backward-propagating photons, respectively as shown in Fig. 2.1.
- The forward-propagating photons travel along z axis and the backward-propagating photons travel along z' axis. We choose y and y' axes to be in the same direction, while x and x' axes to be in the opposite directions.
- A linearly polarized state of a photon with electric field vector along x axis and y axis is represented by $|x\rangle$ and $|y\rangle$, respectively as shown in Fig. 2.2. The relative phase between $|x\rangle$ and $|y\rangle$ is chosen such that $\cos\varphi|x\rangle + \sin\varphi|y\rangle$ represents the state linearly polarized in the

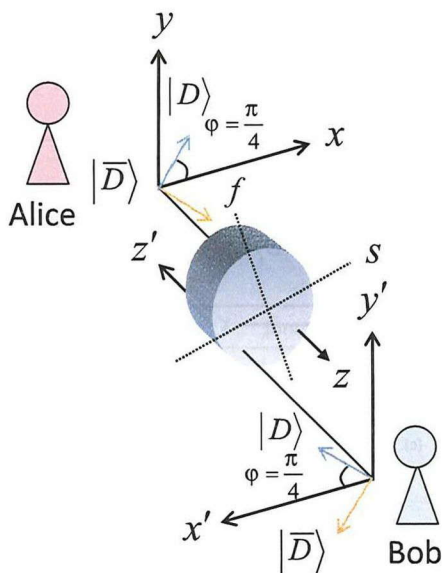


Figure 2.1: Coordinate systems for the forward propagation (xyz) and the backward propagation ($x'y'z'$). Photons propagate along z (z') axis. A birefringent element is located with its surface perpendicular to the z (z') axis.

direction with angle φ from x axis. When $\varphi = \pi/4$ and $-\pi/4$, the states are represented by $|D\rangle$ and $|\bar{D}\rangle$, respectively.

- Using the matrix form, the polarizations are defied as follows.

$$\begin{aligned}
 |x\rangle &= \begin{pmatrix} 1 \\ 0 \end{pmatrix}, & |y\rangle &= \begin{pmatrix} 0 \\ 1 \end{pmatrix} \\
 |D\rangle &= \frac{1}{\sqrt{2}} \begin{pmatrix} 1 \\ 1 \end{pmatrix}, & |\bar{D}\rangle &= \frac{1}{\sqrt{2}} \begin{pmatrix} 1 \\ -1 \end{pmatrix} \\
 |R\rangle &= \frac{1}{\sqrt{2}} \begin{pmatrix} 1 \\ i \end{pmatrix}, & |L\rangle &= \frac{1}{\sqrt{2}} \begin{pmatrix} 1 \\ -i \end{pmatrix}.
 \end{aligned} \tag{2.1}$$

Also the matrices of the polarizers are shown in Fig. 2.3, which is used later.

In quantum communication, informations are encoded into polarization of the photons and they are transmitted using communication channels, usually optical fibers. However, the polarizations are changed during the transmission and initial informations are lost at the receiver's side. Thus, analyzing the changes during the fibers are important. The powerful tool for analyzing the behavior of the polarization is systematically studied by Jones [47, 48]. Using his calculation method, the

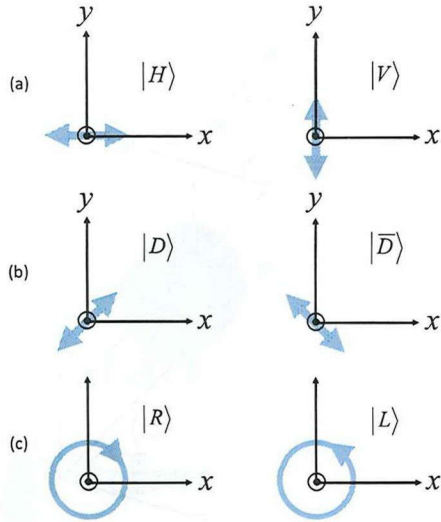


Figure 2.2: Illustration of the polarization states. The propagation direction of the photon is set to $+z$. The polarization is determined by the observer who faces to $-z$. (a) The electric field vector of H polarized state is parallel to x axis and V polarize state is parallel to y axis. (b) D polarized state is just between x and y axes and \bar{D} polarized photon is just between $-x$ and y axes. (c) The electric field of the right-circular polarization is rotated clockwise direction and left-circular polarization is rotated counterclockwise direction.

polarization-state transformations are analyzed.

The media which compose the optical fiber are assumed to have two different crystal axes. These axes are called the slow axis and the fast axis, corresponding to the difference of the refraction indices. Because of this, photons experience the different phases during the traveling the media.

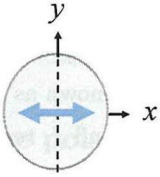
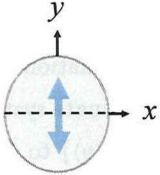
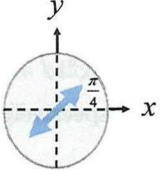
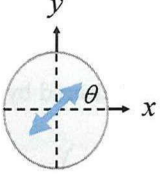
Polarizers	Jones Matrices
	$\begin{pmatrix} 1 & 0 \\ 0 & 0 \end{pmatrix}$
	$\begin{pmatrix} 0 & 0 \\ 0 & 1 \end{pmatrix}$
	$\frac{1}{2} \begin{pmatrix} 1 & 1 \\ 1 & 1 \end{pmatrix}$
	$\begin{pmatrix} \cos^2 \theta & \cos \theta \sin \theta \\ \cos \theta \sin \theta & \sin^2 \theta \end{pmatrix}$

Figure 2.3: The matrices of the polarizers.

2.1.2 Polarization-state transformation in a lossless birefringent element

The aim of this subsection is to analyze the polarization-state transformation in an optical fiber. At first, for simplicity, we analyze the case of one birefringent element. Here we assume a lossless birefringent element. Later we treat a more general case.

A single photon polarization state can be written as

$$\begin{aligned} |\psi\rangle &= V_x|x\rangle + V_y|y\rangle \\ &= \begin{pmatrix} V_x \\ V_y \end{pmatrix}, \end{aligned} \quad (2.2)$$

where V_x and V_y are complex numbers satisfying $|V_x|^2 + |V_y|^2 = 1$. The second line shows the corresponding vector representation of the state, which is known as Jones vector [47, 48]. The slow and fast axis of a birefringent element is represented by s and f , respectively, as shown in Fig. 2.1. The angle between y axis and f axis is θ , where the positive rotation direction is defined to be from positive x (x') axis to positive y (y') axis. The polarization state along s and f axis is represented as $|s\rangle$ and $|f\rangle$, respectively. We first describe the transformation of the polarization state of the forward propagating photon. In this case, we use xyz coordinate system to describe the polarization states. As usual, the transformation of the basis from $\{|x\rangle, |y\rangle\}$ to $\{|s\rangle, |f\rangle\}$ is described as

$$\begin{pmatrix} V_s \\ V_f \end{pmatrix} = \begin{pmatrix} \cos\theta & \sin\theta \\ -\sin\theta & \cos\theta \end{pmatrix} \begin{pmatrix} V_x \\ V_y \end{pmatrix}, \quad (2.3)$$

where V_s and V_f are the coefficients of the $|s\rangle$ and $|f\rangle$, respectively and satisfy $|V_s|^2 + |V_f|^2 = 1$. Here, we define

$$R(\theta) = \begin{pmatrix} \cos\theta & \sin\theta \\ -\sin\theta & \cos\theta \end{pmatrix}. \quad (2.4)$$

After passing through the birefringent element, the state is altered by $|s\rangle \rightarrow e^{-i\phi}|s\rangle$ and $|f\rangle \rightarrow e^{i\phi}|f\rangle$ and described as

$$\begin{pmatrix} V'_s \\ V'_f \end{pmatrix} = \begin{pmatrix} e^{-i\phi} & 0 \\ 0 & e^{i\phi} \end{pmatrix} \begin{pmatrix} V_s \\ V_f \end{pmatrix}. \quad (2.5)$$

V'_x and V'_y are the components of $|x\rangle$ and $|y\rangle$, and we define the phase shift matrix

$$W(\phi) = \begin{pmatrix} e^{-i\phi} & 0 \\ 0 & e^{i\phi} \end{pmatrix}. \quad (2.6)$$

Performing the basis transformation from $\{|s\rangle, |f\rangle\}$ to $\{|x\rangle, |y\rangle\}$ by the rotation matrix $R(-\theta)$, we obtain

$$\begin{pmatrix} V'_x \\ V'_y \end{pmatrix} = \begin{pmatrix} \cos\theta & -\sin\theta \\ \sin\theta & \cos\theta \end{pmatrix} \begin{pmatrix} V'_s \\ V'_f \end{pmatrix}. \quad (2.7)$$

Thus the state after passing through the birefringent element is described as

$$|\psi'\rangle = V'_x|x\rangle + V'_y|y\rangle. \quad (2.8)$$

The overall transformation from initial to final state is described by

$$\begin{aligned} U &\equiv U(\theta, \phi) \\ &= R(-\theta)W(\phi)R(\theta) \\ &= \begin{pmatrix} e^{-i\phi} \cos^2 \theta + e^{i\phi} \sin^2 \theta & -i \sin \phi \sin(2\theta) \\ -i \sin \phi \sin(2\theta) & e^{-i\phi} \sin^2 \theta + e^{i\phi} \cos^2 \theta \end{pmatrix}, \end{aligned} \quad (2.9)$$

where U is a unitary matrix which satisfies $U^\dagger U = \mathbf{1}$ [48].

2.1.3 Examples of the polarization-state transformation 1

We have considered the polarization-state transformation in the birefringent element using Jones calculation method. Here we apply this method to the half-wave plate and the quarter-wave plate.

A half-wave plate

The illustration of the polarization transformation in a half-wave plate is shown in Fig. 2.4. The relative phase retardation of the half-wave plate is π , that is $\phi = \pi/2$. We calculate the output state of the half-wave plate by Jones calculation method. The azimuth angle of the wave plate is taken as $\pi/4$. The matrix of the half-wave plate is written as

$$\begin{aligned} U_{\lambda/2} &= R(-\pi/4)W(\pi/2)R(\pi/4) \\ &= \begin{pmatrix} 0 & -i \\ -i & 0 \end{pmatrix}. \end{aligned} \quad (2.10)$$

When we consider the horizontally polarized state $|x\rangle = \begin{pmatrix} 1 \\ 0 \end{pmatrix}$ as an input state, the output state is described as

$$\begin{aligned} U_{\lambda/2}|x\rangle &= -i \begin{pmatrix} 0 \\ 1 \end{pmatrix} \\ &= -i|y\rangle. \end{aligned} \quad (2.11)$$

The state after passing through the half-wave plate becomes the vertically polarized state. Next we consider right-circular polarized state $|R\rangle = \frac{1}{\sqrt{2}} \begin{pmatrix} 1 \\ i \end{pmatrix}$ as an input state. The output state is

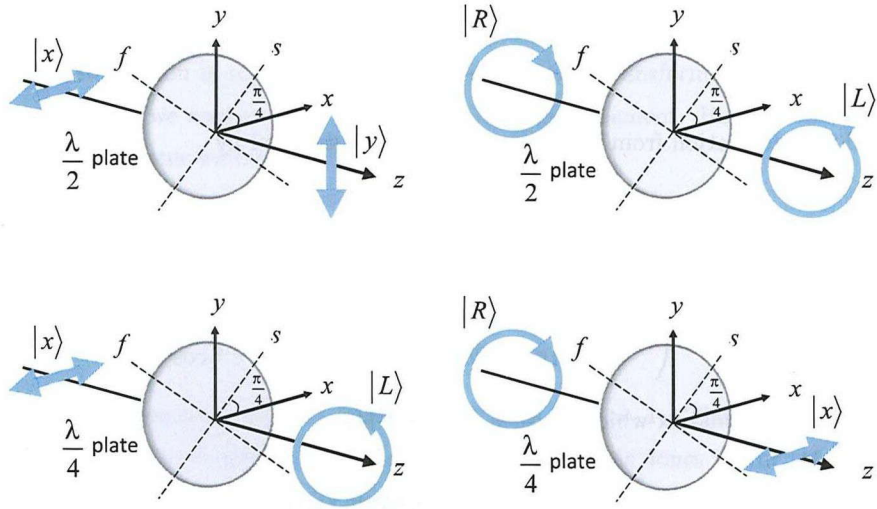


Figure 2.4: Schematic illustration of the polarization transformation in a $\lambda/2$ wave plate (upper) and a $\lambda/4$ wave plate (lower). The angle between the fast axis and y axis is $\pi/4$.

described as

$$\begin{aligned}
 U_{\lambda/2}|R\rangle &= \frac{1}{\sqrt{2}} \begin{pmatrix} 1 \\ -i \end{pmatrix} \\
 &= |L\rangle.
 \end{aligned} \tag{2.12}$$

The output state becomes left-circular polarized state. Note that in case of the circularly polarized state, $|R\rangle$ is transformed into $|L\rangle$ and vice versa, regardless of the azimuth angle.

A quarter-wave plate

In the similar way, we consider the polarization-state transformation in the quarter-wave plate as shown in Fig. 2.4 (lower). The relative phase retardation of the quarter-wave plate is $\pi/2$, that is $\phi = \pi/4$. The azimuth angle of the wave plate is taken as $\pi/4$. The matrix of the quarter-wave plate is written as

$$\begin{aligned}
 U_{\lambda/4} &= R(-\pi/4)W(\pi/4)R(\pi/4) \\
 &= \begin{pmatrix} 1 & -i \\ -i & 1 \end{pmatrix}.
 \end{aligned} \tag{2.13}$$

We consider the horizontally polarized state $|x\rangle = \begin{pmatrix} 1 \\ 0 \end{pmatrix}$ as an input state. Using this expression, the output state is described as

$$\begin{aligned} U_{\lambda/4}|x\rangle &= \frac{1}{\sqrt{2}} \begin{pmatrix} 1 \\ -i \end{pmatrix} \\ &= |L\rangle. \end{aligned} \quad (2.14)$$

The state after passing through the quarter-wave plate is left-circular polarized state. Next we consider right-circular polarized state $|R\rangle = \frac{1}{\sqrt{2}} \begin{pmatrix} 1 \\ i \end{pmatrix}$ as an input state. In this case, the output state is described as

$$\begin{aligned} U_{\lambda/4}|R\rangle &= \frac{1}{\sqrt{2}} \begin{pmatrix} 1 \\ 0 \end{pmatrix} \\ &= |x\rangle. \end{aligned} \quad (2.15)$$

The output state becomes horizontally polarized state. We can easily derive the polarization of the output state after passing through the birefringent element using Jones calculation method.

2.2 Polarization-state transformation in a lossless birefringent elements for the backward-propagating photon

2.2.1 The matrix of the birefringent element for the backward-propagating photon

Let us consider the birefringent effect for the backward propagating photon [49, 50]. In this case, we use $x'y'z'$ coordinate system. Note that the angle between y' and f axis is $-\theta$, as shown Fig. 2.5, while the phase shift matrix is the same. Thus the overall transformation of the photon transmitting from Bob to Alice is described as

$$\begin{aligned} \overleftarrow{U} &\equiv \overleftarrow{U}(\theta, \phi) \\ &= R(\theta)W(\phi)R(-\theta) \\ &= \begin{pmatrix} e^{-i\phi} \cos^2 \theta + e^{i\phi} \sin^2 \theta & i \sin \phi \sin(2\theta) \\ i \sin \phi \sin(2\theta) & e^{-i\phi} \sin^2 \theta + e^{i\phi} \cos^2 \theta \end{pmatrix}. \end{aligned} \quad (2.16)$$

In this thesis \overleftarrow{U} denotes the transformation matrix of the lossless birefringent element for the backward propagating photon described by $x'y'z'$ coordinate system. Using $R(\theta) = ZR(\theta)^T Z$ and

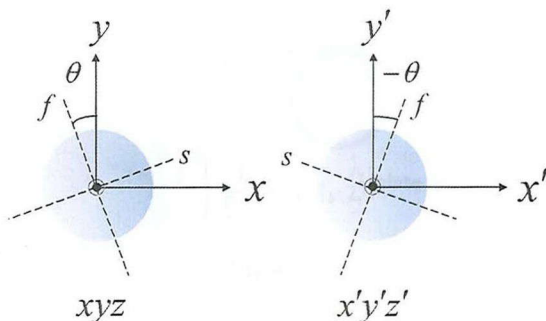


Figure 2.5: The inclination of the f axis in xyz and $x'y'z'$ coordinate systems. The angle between the f axis and the y axis is θ in xyz coordinate system, and $-\theta$ in $x'y'z'$ coordinate system.

$W(\phi) = ZW(\phi)^T Z$, an important relation of the transformations between the forward and the backward propagating photon is found as

$$\overleftarrow{U} = ZU^T Z, \quad (2.17)$$

where Z is a Pauli matrix written as $Z = \begin{pmatrix} 1 & 0 \\ 0 & -1 \end{pmatrix}$. Note that, the selection of the Pauli matrix in (2.17) is changed by the selection of the coordinate system, which is discussed in the Appendix.

2.2.2 Examples of the polarization-state transformation 2

Let us consider some cases of the photon which is propagating toward the backward direction in a birefringent element using $x'y'z'$ coordinate system. In the previous section, we considered the polarization-state transformation in the half-wave plate and the quarter-wave plate for forward propagating photon. In turn, we consider the case where the photon propagates the backward direction, that is to say, the photon enters the birefringent element from the opposite direction.

A half-wave plate

When the $|x\rangle$ state enter the half-wave plate to the forward ($+z$) direction, the output state become $-i|y\rangle$, up to the global phase. Here we consider the case where $-i|y\rangle$ state enter the half-wave plate from the opposite side as shown in Fig. 2.6(a). The matrix of the half-wave plate for the backward propagation is written as

$$\begin{aligned} \overleftarrow{U}_{\lambda/2} &= R(\pi/4)W(\pi/2)R(-\pi/4) \\ &= \begin{pmatrix} 0 & i \\ i & 0 \end{pmatrix}. \end{aligned} \quad (2.18)$$

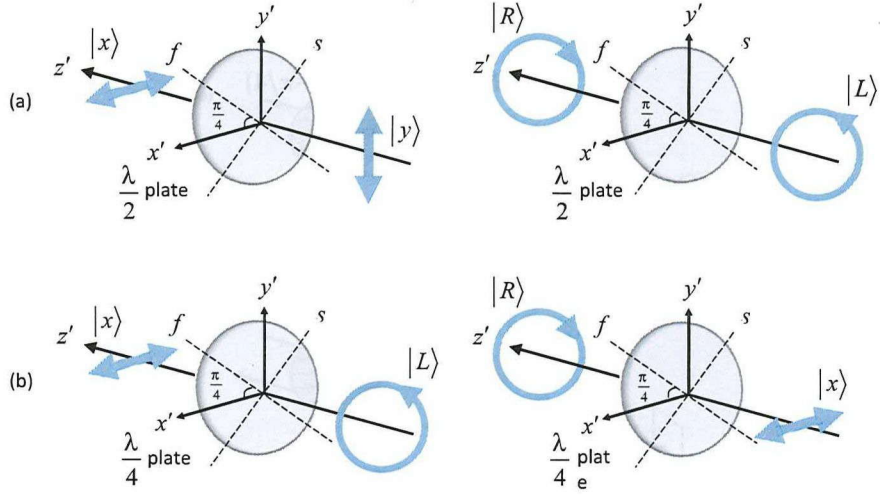


Figure 2.6: Schematic illustration of the polarization transformation in (a) a $\lambda/2$ wave plate and (b) a $\lambda/4$ wave plate. The angle between the fast axis and y axis is $\pi/4$. The photon propagates toward $z'(-z)$ direction.

The polarization state after passing through the element is described as

$$\begin{aligned} \overleftarrow{U}_{\lambda/2}(-i|y\rangle) &= \begin{pmatrix} 1 \\ 0 \end{pmatrix} \\ &= |x\rangle. \end{aligned} \quad (2.19)$$

The state after passing through the half-wave plate is the horizontally polarized state¹. Next we consider left-circular polarized state $|L\rangle$ as an input state. The output state is described as

$$\begin{aligned} \overleftarrow{U}_{\lambda/2}|L\rangle &= \frac{1}{\sqrt{2}} \begin{pmatrix} 1 \\ i \end{pmatrix} \\ &= |R\rangle. \end{aligned} \quad (2.20)$$

The output state becomes right-circular polarized state.

A quarter-wave plate

In the similar way, we consider the polarization-state transformation in the quarter-wave plate for the backward-propagating photon as shown in Fig. 2.6(b). The matrix of the quarter-wave plate for

¹The expression of Eq. (2.19) is the time-reversed version of expression Eq. (2.11). See the next section.

the backward propagation is written as

$$\begin{aligned}\overleftarrow{U}_{\lambda/4} &= R(\pi/4)W(\pi/4)R(-\pi/4) \\ &= \begin{pmatrix} 1 & i \\ i & 1 \end{pmatrix}.\end{aligned}\tag{2.21}$$

We consider the left-circular polarized state $|L\rangle$ as an input state. The output state is described as

$$\begin{aligned}\overleftarrow{U}_{\lambda/4}|L\rangle &= \begin{pmatrix} 1 \\ 0 \end{pmatrix} \\ &= |x\rangle.\end{aligned}\tag{2.22}$$

The state after passing through the quarter-wave plate from the opposite side become horizontally polarized state. Next we consider right-circular polarized state $|x\rangle$ as an input state. In this case, the output state is described as

$$\begin{aligned}\overleftarrow{U}_{\lambda/4}|x\rangle &= \frac{1}{\sqrt{2}} \begin{pmatrix} 1 \\ i \end{pmatrix} \\ &= |R\rangle.\end{aligned}\tag{2.23}$$

The output state becomes right-circular polarized state $|R\rangle$.

Optical isolator based on a birefringent element

The optical device which prevents the backscattered light is called the optical isolator. The schematic picture of the optical isolator based on a birefringent element is shown in Fig. 2.7 (a). The input light is converted into horizontally-polarized light by the linear polarizer, and passes through the quarter-wave plate. After passing the quarter-wave plate, the light is reflected by the mirror. Then the light enters from the opposite side of the quarter-wave plate. At this time, a new coordinate system is introduced so as to the traveling direction of the light is set to $+z'$. The matrix of the isolator is calculated as follows:

$$\begin{aligned}U_{\text{isolator}} &= \overleftarrow{U}_p \overleftarrow{U}_{\lambda/4} U_M U_{\lambda/4} U_p \\ &= \mathbf{0}.\end{aligned}\tag{2.24}$$

The light coming back is blocked completely by the polarizer. Thus the whole system described in Fig. 2.7(a) works as the optical isolator. U_p (\overleftarrow{U}_p) represents the matrix of the polarizer which passes the horizontally-polarized light for forward (backward) propagation, and $U_{\lambda/4}$ ($\overleftarrow{U}_{\lambda/4}$) represents the matrix of the quarter-wave plate which is rotated by $\pi/4$ from the horizontal axis for forward

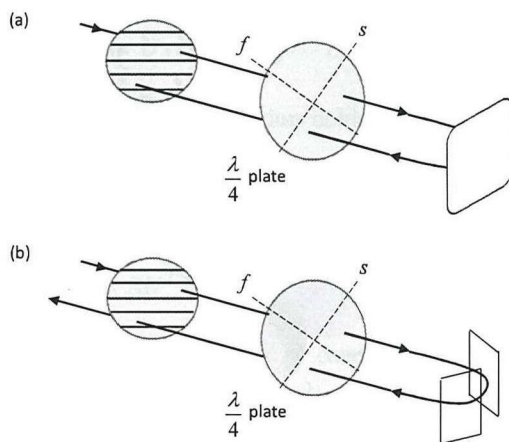


Figure 2.7: Polarization transformation by a $\lambda/4$ wave plate and the reflection by (a) a mirror (b) two mirrors. (a) The light beam coming back after one or odd numbers of reflections are blocked by the linear polarizer, which acts as an isolator. (b) The light beam is not blocked by the linear polarizer and the scheme is not able to isolate the source from the reflected light. Note that the effect of even numbers of mirror reflections equals to the identity operation.

(backward) propagation. The matrix of the polarizer along x axis is represented as $U_p = \overleftarrow{U}_p = \begin{pmatrix} 1 & 0 \\ 0 & 0 \end{pmatrix}$. We have used the relation (2.17) and the matrix of the mirror U_M ², which is represented as

$$U_M = \begin{pmatrix} -1 & 0 \\ 0 & 1 \end{pmatrix} = -Z. \quad (2.25)$$

Next we consider the case where the light is reflected by two mirrors as shown in Fig. 2.7(b). In this case, the matrix representing the whole system is written as

$$U = \overleftarrow{U}_p \overleftarrow{U}_{\lambda/4} U_M U_M U_{\lambda/4} U_p = \begin{pmatrix} 1 & 0 \\ 0 & 0 \end{pmatrix}. \quad (2.26)$$

²The representation of the mirror is related to the two coordinate systems chosen. This is explained in Appendix.

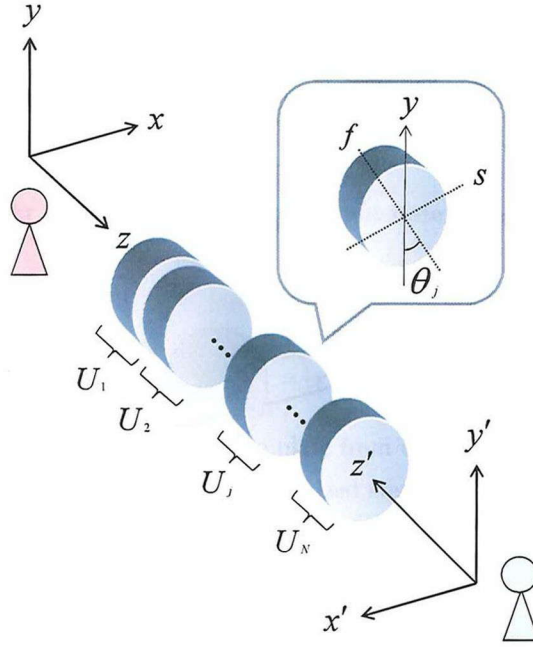


Figure 2.8: A series of birefringent elements as a model of the optical fiber. The angle between f axis and y axis of the j th element is represented by θ_j .

Here the reflected light appears in the input port. These two systems show different behavior by changing the number of the mirrors³. As discussed above, Jones calculation method help us to find out the output state after passing through the optical media and optical devices. When the photon propagates two opposite direction, the state transformation is easily calculated using xyz and $x'Y'a'$ coordinate systems.

2.2.3 The matrix of the optical fiber

We have considered the matrix of a birefringent element for the forward-propagating photon and the backward-propagating photon and derived the relation Eq. (2.17). We now consider more general case, i.e., N birefringent elements as shown Fig. 2.8. The overall matrix of N birefringent elements for the forward propagating photon is described as

$$U = U_N U_{N-1} \cdots U_j \cdots U_2 U_1. \quad (2.27)$$

³The effect of the mirror with odd number reflection is $-Z$, while even number of reflection is $(-Z)^2 = I$.

The subscripts represent j th birefringent element. The corresponding unitary transformation for the backward-propagating photon is written as

$$\overleftarrow{U} = \overleftarrow{U}_1 \overleftarrow{U}_2 \cdots \overleftarrow{U}_j \cdots \overleftarrow{U}_{N-1} \overleftarrow{U}_N. \quad (2.28)$$

Because of the relation (2.17), the following equation holds:

$$\begin{aligned} \overleftarrow{U} &= \overleftarrow{U}_1 \overleftarrow{U}_2 \cdots \overleftarrow{U}_j \cdots \overleftarrow{U}_{N-1} \overleftarrow{U}_N \\ &= Z(U_N U_{N-1} \cdots U_j \cdots U_2 U_1)^T Z \\ &= ZU^T Z. \end{aligned} \quad (2.29)$$

This shows that the relation (2.17) is satisfied in N case. This relation is used in our entanglement distribution protocol since counter-propagating two photons are used in the protocol, which is discussed in Chap. 5.

2.3 Backward propagation and the time-reversal symmetry

In this subsection, we discuss the relation between backward-propagating photon and time-reversed photon. First of all, we briefly review the time-reversal [51].

2.3.1 Antiunitary operator

We define the antiunitary operator θ .

Definition.

The transformation

$$|\alpha\rangle \rightarrow |\bar{\alpha}\rangle = \theta|\alpha\rangle, \quad |\beta\rangle \rightarrow |\bar{\beta}\rangle = \theta|\beta\rangle \quad (2.30)$$

is said to be antiunitary if equations

$$\langle \bar{\beta} | \bar{\alpha} \rangle = \langle \beta | \alpha \rangle^*, \quad (2.31a)$$

$$\theta(c_1|\alpha\rangle + c_2|\beta\rangle) = c_1^*\theta|\alpha\rangle + c_2^*\theta|\beta\rangle \quad (2.31b)$$

are satisfied, for any $\{|\alpha\rangle, |\beta\rangle\}$ and $\{c_1, c_2\}$.

The relation (2.31b) alone defines an antilinear operator. Let us consider the transformation G satisfying

$$|\alpha\rangle \xrightarrow{G} |\bar{\alpha}\rangle. \quad (2.32)$$

The transformations such as spacial inversion and translational operation are examples of them. After the transformation, the absolute value of the inner product, i.e.,

$$|\langle \bar{\beta} | \bar{\alpha} \rangle| = |\langle \beta | \alpha \rangle| \quad (2.33)$$

should be preserved. Concerning this condition, the following theorem (Wigner's theorem) is derived.

Wigner's theorem

Consider the transformation G as following:

$$|\alpha\rangle \xrightarrow{G} |\bar{\alpha}\rangle. \quad (2.34)$$

The condition satisfying (2.33) is either unitarity that satisfies

$$\langle \bar{\beta} | \bar{\alpha} \rangle = \langle U\beta | U\alpha \rangle = \langle \beta | \alpha \rangle \quad (2.35)$$

and

$$U(c_1|\alpha\rangle + c_2|\beta\rangle) = c_1U|\alpha\rangle + c_2U|\beta\rangle, \quad (2.36)$$

or antiunitarity that satisfies

$$\langle \bar{\beta} | \bar{\alpha} \rangle = \langle \theta\beta | \theta\alpha \rangle = \langle \alpha | \beta \rangle = \langle \beta | \alpha \rangle^* \quad (2.37)$$

and

$$\theta(c_1|\alpha\rangle + c_2|\beta\rangle) = c_1^*\theta|\alpha\rangle + c_2^*\theta|\beta\rangle. \quad (2.38)$$

We now claim that an antiunitary operator can be written as

$$\theta = UK, \quad (2.39)$$

where U is a unitary operator and K is the complex-conjugate operator that performs the complex conjugate of any coefficients of states. Before checking (2.31), let us examine the property of the K operator. Suppose we have a state multiplied by a complex number c . Then we have

$$Kc|\alpha\rangle = c^*K|\alpha\rangle. \quad (2.40)$$

Let us consider the case where $|\alpha\rangle$ is expanded in terms of base kets $\{|a'\rangle\}$. Under the action K , we

have

$$\begin{aligned}
|\alpha\rangle &= \sum_{a'} |a'\rangle \langle a'|\alpha\rangle \xrightarrow{K} |\bar{\alpha}\rangle = \sum_{a'} \langle a'|\alpha\rangle^* K|a'\rangle \\
&= \sum_{a'} \langle a'|\alpha\rangle^* |a'\rangle.
\end{aligned} \tag{2.41}$$

This shows that K is antilinear. Since the inner product of $K|\alpha\rangle$ and $K|\beta\rangle$ satisfies $\langle \alpha|\beta\rangle^*$, K is an antiunitary operator. Therefore, we have

$$\begin{aligned}
\theta(c_1|\alpha\rangle + c_2|\beta\rangle) &= \mathcal{U}K(c_1|\alpha\rangle + c_2|\beta\rangle) \\
&= c_1^* \mathcal{U}K|\alpha\rangle + c_2^* \mathcal{U}K|\beta\rangle \\
&= c_1^* \theta|\alpha\rangle + c_2^* \theta|\beta\rangle,
\end{aligned} \tag{2.42}$$

$$\begin{aligned}
|\alpha\rangle &= \sum_{a'} |a'\rangle \langle a'|\alpha\rangle \xrightarrow{\theta} |\bar{\alpha}\rangle = \sum_{a'} \langle a'|\alpha\rangle^* \mathcal{U}K|a'\rangle \\
&= \sum_{a'} \langle a'|\alpha\rangle^* \mathcal{U}|a'\rangle
\end{aligned}$$

and

$$|\bar{\beta}\rangle = \sum_{a'} \langle a'|\beta\rangle^* \mathcal{U}|a'\rangle \stackrel{\text{DC}}{\leftrightarrow} \langle \bar{\beta}| = \sum_{a'} \langle a'|\beta\rangle \langle a'|\mathcal{U}^\dagger. \tag{2.43}$$

These properties clearly show

$$\begin{aligned}
\langle \bar{\beta}|\bar{\alpha}\rangle &= \sum_{a''} \sum_{a'} \langle a''|\beta\rangle \langle a''|\mathcal{U}^\dagger \mathcal{U}|a'\rangle \langle \alpha|a'\rangle \\
&= \sum_{a'} \langle \alpha|a'\rangle \langle a'|\beta\rangle = \langle \alpha|\beta\rangle \\
&= \langle \beta|\alpha\rangle^*.
\end{aligned} \tag{2.44}$$

Thus $\theta = \mathcal{U}K$ is an antiunitary operator.

2.3.2 Time-reversal operator

In many situations of physics, the time-reversal phenomena is discussed. The arrow of time is one way, however, in many cases, we can not discriminate whether it is real-time event or time-reverse version of it. Imagine the case where you are looking the film. In the film, the ball with parabolic motion is taken⁴. Is it possible for you to distinguish whether you are looking the film with right motion or reversed motion? The answer is no, since both of the motions in the film satisfies the equation of motion, i.e, both of the motions are physically correct. More formally, if $\mathbf{x}(t)$ is a solution to

$$m\ddot{\mathbf{x}} = -\nabla V(\mathbf{x}), \tag{2.45}$$

⁴In this situation, the effect of the air resistance is neglected.

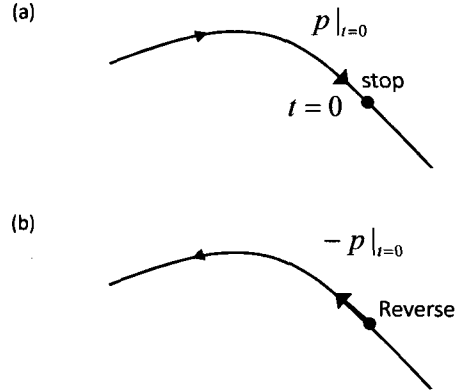


Figure 2.9: Illustration of the trajectory of the classical particle. (a) The time-reversal operation is applied at time $t = 0$, (b) then the particle is reversed its direction. The particle which is applied the operation traces the same trajectory in the opposite direction.

then $\mathbf{x}(-t)$ is also a possible solution in the same force field derivable from V . In general, if the system has the time-reversal symmetry, we can not distinguish whether time flows toward the future or the past. The time-reversal operator is such a operator that reverse the time toward the past. Let us denote the time-reversal operator by \mathcal{T} , which is an antiunitary operator. Consider

$$|\alpha\rangle \rightarrow \mathcal{T}|\alpha\rangle, \quad (2.46)$$

where $|\alpha\rangle$ is the quantum state and $\mathcal{T}|\alpha\rangle$ is the time-reversed state of $|\alpha\rangle$. If the $|\alpha\rangle$ is a momentum eigenstate $|p\rangle$, we expect $\mathcal{T}|p\rangle$ to be $-|p\rangle$ up to a possible phase.

We now consider the property of the time-reversal operator by looking at the evolution of the time-reversed state. Consider a physical system represented by $|\alpha\rangle$ at $t = 0$. Then at a slightly later time $t = \delta t$, the system is found in

$$|\alpha; t = \delta t\rangle = \left(1 - \frac{iH}{\hbar}\delta t\right)|\alpha\rangle, \quad (2.47)$$

where H is the Hamiltonian that characterize the time evolution. Suppose we apply \mathcal{T} at $t = 0$, and then let the system evolves under the influence of the Hamiltonian H . We then have at δt

$$\left(1 - \frac{iH}{\hbar}\delta t\right)\mathcal{T}|\alpha\rangle. \quad (2.48)$$

If the motion obeys symmetry under time reversal, we *expect* the preceding state to be the same as

$$\mathcal{T}|\alpha; t = -\delta t\rangle \quad (2.49)$$

that is, first consider a state at earlier time $t = -\delta t$, and then reverse the motion; see Fig. 2.10. Mathematically,

$$\left(1 - \frac{iH}{\hbar}\delta t\right)\mathcal{T}|\alpha\rangle = \mathcal{T}\left(1 - \frac{iH}{\hbar}(-\delta t)\right)|\alpha\rangle. \quad (2.50)$$

If the relation is satisfied by any state, we must have

$$-iHT|\cdot\rangle = \mathcal{T}iH|\cdot\rangle, \quad (2.51)$$

where $|\cdot\rangle$ means any state.

We now argue that \mathcal{T} *cannot* be unitary if the motion of time reversal is to make sense. Suppose \mathcal{T} were unitary. It would then be legitimate to cancel the i 's in (2.51), and we would have the operator equation

$$-HT = \mathcal{T}H. \quad (2.52)$$

Consider an energy eigen state $|n\rangle$ with energy eigenvalue E_n . The corresponding time-reversed state would be $\mathcal{T}|n\rangle$, and we would

$$HT|n\rangle = -\mathcal{T}H|n\rangle = (-E_n)\mathcal{T}|n\rangle. \quad (2.53)$$

This equation says that $\mathcal{T}|n\rangle$ is an eigen state of the Hamiltonian with energy eigenvalue $-E_n$, however this eigen value should be positive. Consider the free-particle Hamiltonian. We expect \mathbf{p} to change the sign but not \mathbf{p}^2 , yet (2.52) would imply that

$$\mathcal{T}^{-1}\frac{\mathbf{p}^2}{2m}\mathcal{T} = \frac{-\mathbf{p}^2}{2m}. \quad (2.54)$$

All these arguments suggest that if time reversal is to be sensitive, \mathcal{T} should be antiunitary. In this case the right-hand side of (2.51) becomes

$$\mathcal{T}iH|\cdot\rangle = -i\mathcal{T}H|\cdot\rangle \quad (2.55)$$

by anti-linear property. Now at last we can cancel i 's in (2.51) leading to

$$\mathcal{T}H = H\mathcal{T}. \quad (2.56)$$

This relation expresses the fundamental property of the Hamiltonian under time reversal. With this equation the difficulties mentioned earlier [(2.52) to (2.54)] are absent, and we obtain physically sensible results. From now on we will always take \mathcal{T} to be antiunitary.

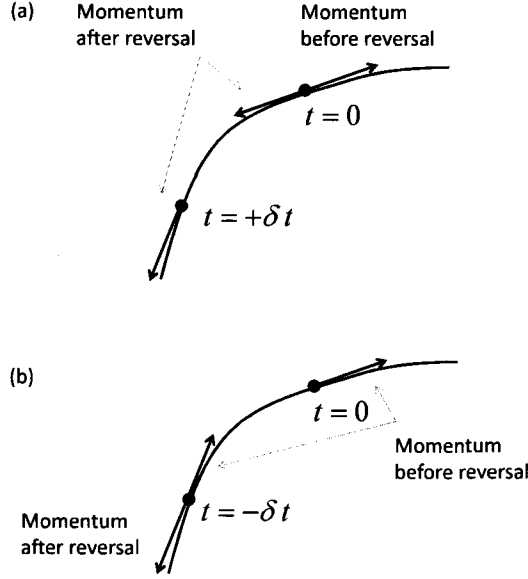


Figure 2.10: Schematic drawing of the motion before and after time reversal at time $t = 0$ and $t = \pm\delta t$. (a) Time is reversed at $t = 0$ and then the system evolves δt . (b) Time evolves $-\delta t$ then time is reversed. If the time-reversal symmetry holds, the motion in (a) and (b) should correspond, i.e., Eq. (2.50) holds.

2.3.3 Relation between backward propagation and the time-reversal symmetry

Here we suppose that $|\phi\rangle$ is the input state and $|\psi\rangle$ is the output state after passing through the birefringent media. Then the relation

$$|\psi\rangle = U|\phi\rangle \quad (2.57)$$

holds. U is a unitary matrix for the birefringent media. Next let us consider the situation when the time is reversed⁵. The output photon will retrace the birefringent media. In this case, the output state with the time-reversal operator becomes the input state which enters from the opposite side of the birefringent media as shown in Fig. 2.11. Such a state is described by $\mathcal{T}|\psi\rangle$, where \mathcal{T}

⁵When the time-reversal is considered, we have to suppose a lossless channel. If not, we have to permit the leak up of the photon.

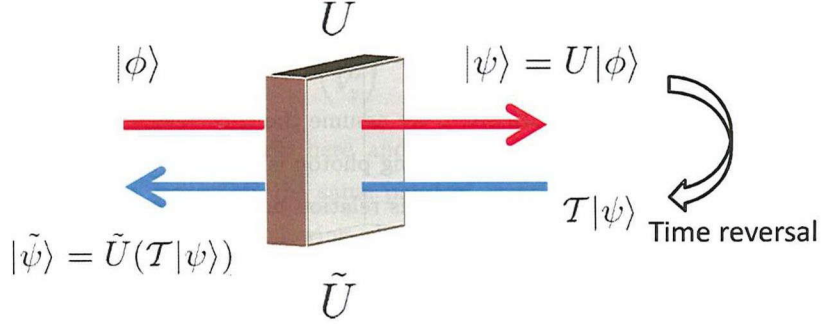


Figure 2.11: Illustration of the input-output state (red line) and time-reversed version of it (blue line). Eq. (2.29) is derived using the time-reversal symmetry.

represents the time-reversal operator. As discussed, the time reversal operator \mathcal{T} is written by the product of a unitary operator \mathcal{U} and the conjugation operator K , i.e., $\mathcal{T} = \mathcal{U}K$. In this situation, \mathcal{U} corresponds to the matrix $-Z$, which transform the coordinate system for forward propagation into that of backward propagation⁶. Hereafter we define the time-reversal operator as

$$\mathcal{T} = -ZK. \quad (2.58)$$

Then the time-reversed state $\mathcal{T}|\psi\rangle$ enters the birefringent media from the opposite side (right side in Fig. 2.11) and the state after passing through the media is described as

$$|\tilde{\psi}\rangle = \tilde{U}(\mathcal{T}|\psi\rangle), \quad (2.59)$$

where \tilde{U} is the matrix of the birefringent media from the opposite side. If the time-reversal symmetry holds, $|\tilde{\psi}\rangle$ should correspond to $\mathcal{T}|\phi\rangle$, which is time-reversed state of the input state $|\phi\rangle$. That is to say, the relation

$$\begin{aligned} |\tilde{\psi}\rangle &= \mathcal{T}|\phi\rangle \\ \Leftrightarrow \mathcal{T}|\phi\rangle &= \tilde{U}\mathcal{T}U|\phi\rangle \end{aligned} \quad (2.60)$$

⁶When the time is reversed, the propagation direction of the photon is also reversed. In such a case, in our definition, $x'y'z'$ coordinate system is introduced.

holds. This relation leads to

$$\begin{aligned}\tilde{U} &= \mathcal{T}U^\dagger\mathcal{T}^{-1} \\ &= ZU^T Z,\end{aligned}\tag{2.61}$$

which corresponds to (2.17)⁷. Interestingly, if we assume the time-reversal symmetry, the relation for forward-propagating and backward-propagating photon is derived⁸.

Using simple example, let us confirm that this relation holds. As an input state, we introduce $|\phi\rangle = |x\rangle$, and we consider $U_{\lambda/4} = \begin{pmatrix} 1 & -i \\ -i & 1 \end{pmatrix}$ as the transformation matrix of the media. The output state after transmitting the media becomes

$$\begin{aligned}|\psi\rangle &= U_{\lambda/4}|x\rangle \\ &= |L\rangle.\end{aligned}\tag{2.62}$$

Let us consider the case when the time is reversed. Operating \mathcal{T} on $|\psi\rangle = |L\rangle$ the state becomes $\mathcal{T}|\psi\rangle = -ZK|L\rangle = -|L\rangle$, which is the input state entering from the opposite side. After passing through the media, the state is described as

$$\begin{aligned}|\tilde{\psi}\rangle &= \tilde{U}_{\lambda/4}(-|L\rangle) \\ &= -|x\rangle.\end{aligned}\tag{2.63}$$

On the other hand, operating \mathcal{T} on the initial input state, the state become $\mathcal{T}|x\rangle = -|x\rangle$, which is the same as (2.63) up to the global phase. This means that the relation (2.61) derived from the time-reversal symmetry corresponds to the matrix for the backward propagation, i.e., $\tilde{U} = \overleftarrow{U}$.

2.4 Polarization-state transformation in reciprocal media

In the previous subsections, we have considered the polarization-state transformation in multiple birefringent elements. Here we consider more general case whose optical fiber is composed a sequence of birefringent elements with polarization dependent photon losses. In order to analyze such media, we extend the definition of the vector representation to the case where $P(V_x, V_y) \equiv |V_x|^2 + |V_y|^2 < 1$, such that it represents the state whose density operator is $\rho(V_x, V_y) \equiv (1 - P(V_x, V_y))|0\rangle\langle 0| + |\psi\rangle\langle\psi|$. Here $|0\rangle$ is the vacuum and $|\psi\rangle$ is given by Eq. (2.2). Then, the effect of any linear passive optical

⁷This relation is true for the case of N birefringent elements.

⁸In some references, the matrix for the backward propagation is written as $\tilde{U} = U^T$. In their definition, no coordinate transformation is performed. In other word, the direction of $+z$ is fixed despite of the change of the propagation direction of the photon. In such case, \mathcal{U} equals to I , and $\mathcal{T} = K$.

component is represented by a complex matrix M satisfying $M^\dagger M \leq \mathbf{1}$, which transforms the input state $\rho(V_x, V_y)$ to the output state $\rho(V'_x, V'_y)$ as

$$\begin{pmatrix} V'_x \\ V'_y \end{pmatrix} = M \begin{pmatrix} V_x \\ V_y \end{pmatrix}. \quad (2.64)$$

We call M a transformation matrix here and henceforth. Note that, since $\rho(e^{i\phi}V_x, e^{i\phi}V_y) = \rho(V_x, V_y)$, M and $e^{i\phi}M$ represents the same physical transformation. Using such media, the polarization state is altered by the following phase shifts and polarization dependent photon losses as $|s\rangle \rightarrow \gamma_s e^{-i\phi}|s\rangle$ and $|f\rangle \rightarrow \gamma_f e^{i\phi}|f\rangle$, where γ_s and γ_f are non-negative real numbers satisfying $\gamma_s \leq 1$ and $\gamma_f \leq 1$. Here the polarization state along s and f axis is represented by $|s\rangle$ and $|f\rangle$, respectively, where

$$|s\rangle = \cos\theta|x\rangle + \sin\theta|y\rangle, \quad (2.65)$$

and

$$|f\rangle = -\sin\theta|x\rangle + \cos\theta|y\rangle. \quad (2.66)$$

Thus the phase shift matrix (2.6) is modified to

$$W(\gamma_s, \gamma_f, \phi) = \begin{pmatrix} \gamma_s e^{-i\phi} & 0 \\ 0 & \gamma_f e^{i\phi} \end{pmatrix}. \quad (2.67)$$

In a similar way, as discussed before, the transformation matrix M is written in the $\{|x\rangle, |y\rangle\}$ basis as

$$\begin{aligned} M &= R(-\theta)W(\gamma_s, \gamma_f, \phi)R(\theta) \\ &= \begin{pmatrix} \gamma_s e^{-i\phi} \cos^2\theta + \gamma_f e^{i\phi} \sin^2\theta & (\gamma_s e^{-i\phi} - \gamma_f e^{i\phi}) \sin\theta \cos\theta \\ (\gamma_s e^{-i\phi} - \gamma_f e^{i\phi}) \sin\theta \cos\theta & \gamma_s e^{-i\phi} \sin^2\theta + \gamma_f e^{i\phi} \cos^2\theta \end{pmatrix}. \end{aligned} \quad (2.68)$$

The transformation matrix for backward propagation \overleftarrow{M} is derived using $x'y'z'$ coordinate system, in the same manner, since the phase shift matrix (2.67) stays unchanged. This leads to

$$\begin{aligned} \overleftarrow{M} &= R(\theta)W(\gamma_s, \gamma_f, \phi)R(-\theta) \\ &= \begin{pmatrix} \gamma_s e^{-i\phi} \cos^2\theta + \gamma_f e^{i\phi} \sin^2\theta & -(\gamma_s e^{-i\phi} - \gamma_f e^{i\phi}) \sin\theta \cos\theta \\ -(\gamma_s e^{-i\phi} - \gamma_f e^{i\phi}) \sin\theta \cos\theta & \gamma_s e^{-i\phi} \sin^2\theta + \gamma_f e^{i\phi} \cos^2\theta \end{pmatrix}. \end{aligned} \quad (2.69)$$

Therefore the same relation

$$\overleftarrow{M} = ZM^T Z \quad (2.70)$$

is obtained. In general, M is not a unitary matrix. The equation $ZM^T Z = XM^\dagger X$ is satisfied when $\gamma_s = \gamma_f = 1$. It is noticed that the relation (2.70) (also (2.17)) can be represented by $\overleftarrow{M} = U_R M^T U_R^\dagger$ ($\overleftarrow{U} = U_R U^T U_R^\dagger$) with unitary matrix U_R , where $U_R = R(\alpha)Z$ and α depends on the coordinate systems chosen [49, 50].

The above relation of the single-element transformation between forward and backward propagation is easily extended to N elements in a similar way discussed before. Suppose that the overall transformation matrix of the sequence of N birefringent elements for a forward-propagating photon is given by

$$M = M_N M_{N-1} \cdots M_j \cdots M_2 M_1, \quad (2.71)$$

where M_j stands for the transformation matrix of the j th birefringent element. The corresponding transformation matrix for a backward-propagating photon is written as

$$\overleftarrow{M} = \overleftarrow{M}_1 \overleftarrow{M}_2 \cdots \overleftarrow{M}_j \cdots \overleftarrow{M}_{N-1} \overleftarrow{M}_N. \quad (2.72)$$

Because of the relation (2.70), the following equation holds:

$$\begin{aligned} \overleftarrow{M} &= \overleftarrow{M}_1 \overleftarrow{M}_2 \cdots \overleftarrow{M}_j \cdots \overleftarrow{M}_{N-1} \overleftarrow{M}_N \\ &= Z(M_N M_{N-1} \cdots M_j \cdots M_2 M_1)^T Z \\ &= ZM^T Z. \end{aligned} \quad (2.73)$$

This clearly shows that the relation (2.70) is satisfied by a composite system of the birefringent elements with polarization dependent photon losses. The relation 2.73 is used in our entanglement distribution protocol in Chap. 5.

2.5 The universal compensator

In the previous section, we summarize the polarization state transformation by a composite birefringent element and present the relation of its transformation between forward and backward propagation through a reciprocal media. In order to see the usefulness of the relation (2.17), we apply it to an explanation of the universal compensator proposed by Martinelli [52]. The universal compensator is used for a cancellation of polarization state transformation by fluctuations in a reciprocal media, which is the essence of Plug and Play QKD protocol [26, 53]. However widely known explanation of the working principle of the protocol is done using the right-handed coordinate system for the forward propagation and the left handed coordinate system for the backward propagation, which leads to a confusion when we consider a manipulation of a part of composite quantum systems. On the other hand, in the previous chapter, the coordinate systems are fixed to be right-handed for both propagation direction. In this chapter, we reconstruct the working principle of the universal compensator using our definition, which make the understanding easily.

2.5.1 The universal compensator

The apparatus which is used in the universal compensator is composed of only magnetic media which induce the Faraday rotation and a plane mirror. Before describing the Martinelli's universal compensator, we first review the state transformation by the Faraday rotator [48].

The Faraday mirror

The natural propagating mode in the magnetic media is circular polarization state, i.e., right-circular $|R\rangle = \frac{1}{\sqrt{2}}(|x\rangle + i|y\rangle)$ and left-circular $|L\rangle = \frac{1}{\sqrt{2}}(|x\rangle - i|y\rangle)$ polarized state. These circular polarization state propagate with different phase velocity in the media. In other words, the phase shift during such media is diagonalized in the $\{|R\rangle, |L\rangle\}$ basis. This causes the Faraday rotation. The state transformation by the Faraday rotator is described as follows: During a photon propagates through magnetic media, right-circular polarized photon and left-circular polarized photon experience the phase shift $|R\rangle \rightarrow e^{i\theta_F}|R\rangle$ and $|L\rangle \rightarrow e^{-i\theta_F}|L\rangle$. Output state after transmitting the magnetic media becomes

$$\begin{pmatrix} V'_R \\ V'_L \end{pmatrix} = \begin{pmatrix} e^{i\theta_F} & 0 \\ 0 & e^{-i\theta_F} \end{pmatrix} \begin{pmatrix} V_R \\ V_L \end{pmatrix}, \quad (2.74)$$

where V_R, V_L, V'_R and V'_L are the components of $|R\rangle$ and $|L\rangle$. We define the phase shift matrix of the magnetic media $W_F(\theta_F) = \begin{pmatrix} e^{i\theta_F} & 0 \\ 0 & e^{-i\theta_F} \end{pmatrix}$. The basis transformation $\{|x\rangle, |y\rangle\}$ to $\{|R\rangle, |L\rangle\}$ is written as

$$\begin{aligned} \begin{pmatrix} V_R \\ V_L \end{pmatrix} &= \frac{1}{2} \begin{pmatrix} 1 & i \\ 1 & -i \end{pmatrix} \begin{pmatrix} V_x \\ V_y \end{pmatrix} \\ &= T \begin{pmatrix} V_x \\ V_y \end{pmatrix}, \end{aligned} \quad (2.75)$$

while the reverse transformation is described as

$$\begin{pmatrix} V_x \\ V_y \end{pmatrix} = T^{-1} \begin{pmatrix} V_R \\ V_L \end{pmatrix}. \quad (2.76)$$

Thus the output state is written as

$$\begin{aligned}
\begin{pmatrix} V'_x \\ V'_y \end{pmatrix} &= T^{-1} W_F(\theta_F) T \begin{pmatrix} V_x \\ V_y \end{pmatrix} \\
&= \begin{pmatrix} \cos \theta_F & -\sin \theta_F \\ \sin \theta_F & \cos \theta_F \end{pmatrix} \begin{pmatrix} V_x \\ V_y \end{pmatrix} \\
&= R(-\theta_F) \begin{pmatrix} V_x \\ V_y \end{pmatrix}.
\end{aligned} \tag{2.77}$$

When the linearly polarized photons enter the Faraday rotator, the output photons are linearly polarized and rotated by θ_F ⁹. In the same way, we consider the Faraday rotation for backward propagating photon. In this case, the photon is rotated by $-\theta_F$ on $x'y'z'$ coordinate system since the direction of magnetic field is contrary to that of the backward propagating photon. The rotation matrix for the photon is described as

$$\begin{aligned}
T^{-1} W_F(-\theta_F) T &= \begin{pmatrix} \cos \theta_F & \sin \theta_F \\ -\sin \theta_F & \cos \theta_F \end{pmatrix} \\
&= R(\theta_F).
\end{aligned} \tag{2.78}$$

Note that the polarization is always rotated by the same direction regardless of its propagation direction.

The Faraday mirror is composed of the Faraday rotator with $\theta_F = \pi/4$ and a plain mirror. After passing through the Faraday rotator, a photon is reflected by the mirror. The matrix of a plain mirror is expressed by $-Z = \begin{pmatrix} -1 & 0 \\ 0 & 1 \end{pmatrix}$. After the reflection, the photon passes through the Faraday rotator again. Eventually, the photon is rotated by $-\pi/4$. The overall transformation of the Faraday mirror is described as

$$\begin{aligned}
U_{FM} &= R(\pi/4)(-Z)R(-\pi/4) \\
&= \begin{pmatrix} 0 & 1 \\ 1 & 0 \end{pmatrix} = X.
\end{aligned} \tag{2.79}$$

Universal compensator

We describe Martinelli's universal compensator of a polarization state over the reciprocal media. The universal compensator is achieved by an additional Faraday mirror at the end of the reciprocal media

⁹It is noticed that in our notation, $R(\theta)$ means the rotation of the coordinate system counterclockwise direction. This means that the polarization state (vector) is rotated $-\theta$ (clockwise direction).

by using relation (2.17). A photon passing through the reciprocal media is reflected by the Faraday mirror, and goes back to the sender through the reciprocal media. The overall transformation is written as

$$\begin{aligned}
U_{\text{total}} &= \overleftarrow{U} U_{\text{FM}} U \\
&= (XU^\dagger X) X U \\
&= X.
\end{aligned} \tag{2.80}$$

In the second line, we have used $\overleftarrow{U} = ZU^T Z = XU^\dagger X$. The result shows that any transformation acting on the polarization states caused by the slowly fluctuating reciprocal media is eliminated, except for the transmittance of the photon and the effect of Faraday rotator.

At last, we consider the universal compensator against an optical fiber with polarization dependent photon losses. In this case, the overall transformation is written as

$$\begin{aligned}
M_{\text{total}} &= \overleftarrow{M} U_{\text{FM}} M \\
&= (ZM^T Z) X M \\
&= (\det M) X.
\end{aligned} \tag{2.81}$$

The extra coefficient $\det M$ is added compared to (2.80). Using the relation (2.70) (also (2.17)) reproduce the same result shown by Martinelli and is applied to Plug and Play QKD proposed by Muller *et al.* [53, 26].

Other application of the Faraday mirror - an optical isolator -

As discussed in 2.2.2, the isolator play a role of blocking the backward scattering light. In this subsection we refocus on the isolator, which includes the magnetic media this. The structure of the isolator is shown as follows: The input light (forward-propagating) beam passes through the linear polarizer which get through horizontally polarized beam, then the polarization (vector) of the light beam is rotated $\pi/4$ by Faraday rotator, which is made of the magnetic media as shown in Fig. 2.12. Looking the light from the observer who faces the coming light, the light is rotated counterclockwise direction, which is represented by $R(-\pi/4)$ using xyz coordinate system¹⁰. The 45-degree light polarizer is set after the magnetic media, which passes all the beam. Next we consider the backward-propagating light which progress the same route toward the reverse direction. This situation can be realized by reflecting the input light using a mirror. We call this light backscattering light. Then the back scattering light is rotated $-\pi/4$. Looking the light from another observer who faces the mirror, the polarization (vector) of the backscattering light is rotated clockwise direction,

¹⁰Be careful of the difference between the rotation of the coordinate system and the rotation of the polarization (vector).

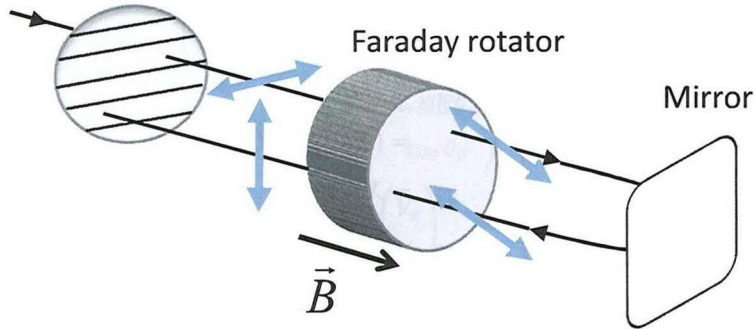


Figure 2.12: Illustration of the optical isolator with Faraday rotation. The reflected light is absorbed by the polarizer.

which is represented $R(\pi/4)$ using $x'y'z'$ coordinate system¹¹. The light after passing through the magnetic media becomes vertically polarized light beam. The total effect of the isolator is described as

$$\begin{aligned}
 U_{\text{isolator}} &= \overleftarrow{U}_p R(\pi/4) U_M R(-\pi/4) U_p \\
 &= \mathbf{0},
 \end{aligned} \tag{2.82}$$

which means that the backscattering light is blocked completely. We have used $U_p = \begin{pmatrix} 1 & 0 \\ 0 & 0 \end{pmatrix}$, $U_M = \begin{pmatrix} -1 & 0 \\ 0 & 1 \end{pmatrix}$ and the relation $\overleftarrow{U}_p = Z U_p^T Z$.

2.6 discussion

In our definition, $+z$ axis is always set to the propagation direction of the photon. Thus in case of treating photons which are counter-propagating each other, we have introduced two coordinate systems depending on the propagation directions of the photons. However, this is not the only way to deal such photons with. One of the idea is to use just one coordinate system regardless of the propagation directions of the photons. In this case, we do not care the propagation direction of the photon and xyz coordinate system is always fixed. The definition of polarization-state used here is as follows:

¹¹If the same observer sees this, the light is rotated the same direction regardless of the propagation direction.

- Unlike our style, only one coordinate system xyz is used. The forward-propagating photon propagates along the $+z$ axis and the backward-propagating photon propagates toward $-z$.
- The polarization of the photon is defined by the observer who looks the photon coming.
- A linearly polarized state of a photon with electric field vector along x axis and y axis is represented by $|x\rangle$ and $|y\rangle$, respectively as shown in Fig. 2.2(a). Regardless of the propagation direction, an electric field vector just between x and y axis and just between $-x$ and y axis are represented by $|D\rangle$ and $|\bar{D}\rangle$, respectively.
- Cautions are required for the definition of circular-polarized photon state. The electric vector of $|R\rangle$ and $|L\rangle$ circular-polarized photon is always rotating the same direction. Regardless of the propagation direction, the electric vector of $|R\rangle$ circular-polarized state is rotating toward $+y$ to $+x$ axis, while the electric vector of $|L\rangle$ circular-polarized state is rotating toward $+y$ to $-x$ axis.

We now consider the polarization transformation in a birefringent element for forward-propagating photon and backward propagating photon as shown in Fig. 2.13. For simplicity, we neglect the polarization dependent photon loss. As shown, the matrix of the birefringent element for forward-propagating photon is described as

$$\begin{aligned}
 U' &= R(-\theta)W(\phi)R(\theta) \\
 &= \begin{pmatrix} e^{-i\phi} \cos^2 \theta + e^{i\phi} \sin^2 \theta & -i \sin \phi \sin(2\theta) \\ -i \sin \phi \sin(2\theta) & e^{-i\phi} \sin^2 \theta + e^{i\phi} \cos^2 \theta \end{pmatrix}, \tag{2.83}
 \end{aligned}$$

which is same as Eq. (2.9). Next we evaluate the matrix for backward-propagating photon. In this notation, as shown Fig. 2.14, the angle between y and f axis is still θ , since x and y axes are fixed¹². Thus the matrix is described as

$$\begin{aligned}
 \overleftarrow{U}' &= R(-\theta)W(\phi)R(\theta) \\
 &= \begin{pmatrix} e^{-i\phi} \cos^2 \theta + e^{i\phi} \sin^2 \theta & -i \sin \phi \sin(2\theta) \\ -i \sin \phi \sin(2\theta) & e^{-i\phi} \sin^2 \theta + e^{i\phi} \cos^2 \theta \end{pmatrix}. \tag{2.84}
 \end{aligned}$$

The relation of these matrices are derived as

$$\begin{aligned}
 \overleftarrow{U}' &= R(-\theta)W(\phi)R(\theta) \\
 &= R(\theta)^T W(\phi)^T R(-\theta)^T \\
 &= (R(-\theta)W(\phi)R(\theta))^T \\
 &= U'^T, \tag{2.85}
 \end{aligned}$$

¹²Positive rotation direction is defied $+x$ to $+y$.

which is different representation from (2.17). T represents the transposition of the matrix. This relation is easily generalized to N birefringent elements case using the same way as discussed.

The cause of the difference between (2.17) and (2.85) is connected to the choice of the coordinate systems. In the former case, two coordinate systems are introduced and y and y' axes are chosen to be the same direction. On the other hand, in the latter case, only one coordinate system is introduced. The choice of the coordinate systems leads the different relation between forward- and backward-propagating photon.

2.7 Summary

In conclusion, we have considered the polarization-state transformation in a birefringent element using Jones calculation method, and moreover, it is generalized to an optical fiber which is composed of N birefringent elements. This calculation method enables us to analyze the output state from an optical fiber easily when the input state is given. More importantly, the relation of the birefringent media between forward- and backward-propagating photons (2.73) is derived. With respect to the derivation of this relation, we have used two coordinate systems depending on the propagation direction of the photon. In order to see the usefulness of this relation, we have applied it to an explanation of the universal compensator and its application Plug and Play QKD. The merit of using our system is that the polarization-state is defined by the right-handed coordinate systems despite of the propagation direction of the photons. This enables us to easily understand the polarization transformation of photons which propagate the opposite direction and used in newly proposed entanglement distribution scheme in Chapter 5.

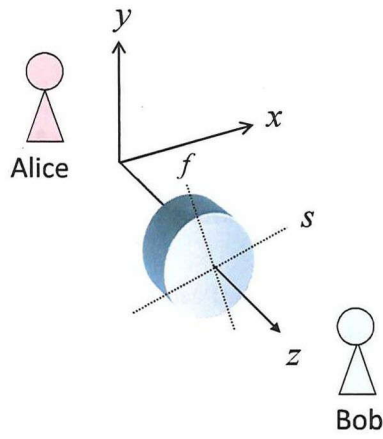


Figure 2.13: Polarization transformation of the forward- and backward-propagating photon by single coordinate system.

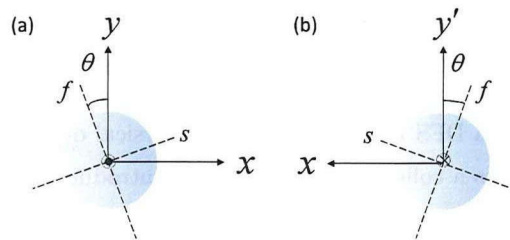


Figure 2.14: Illustration of the angle between f axis and y axis. The same coordinate system is used. The positive direction of the rotation is defined $+x$ axis to $+y$ axis.

Chapter 3

Quantum communication based on the DFS

Faithful qubit distribution among distantly located Alice (sender) and Bob (receiver) is an important issue in the quantum communication. However, because of the coupling with the environmental systems, which are the causes of the channel noises, initial state is destroyed during the transmission. One of the promising noise suppressing method to overcome such a problem is encoding qubits into *noiseless subspace*, called DFS [29, 30]. The DFS is a part of the Hilbert space and qubits are encoded within the states spanned by this subspace. In this chapter, we introduce some photonic qubit distribution protocols based on the DFS.

3.1 Introduction to the DFS based quantum communication

Logical qubits embedded in a DFS formed by multiple physical qubits is immune to a class of the noises, which is referred to as a collective noise. We first introduce a DFS formed by two physical qubits for a collective phase noise channel. Following the convention, hereafter we use the notation of the basis $\{|H\rangle, |V\rangle\}$ instead of $\{|x\rangle, |y\rangle\}$, where $|H\rangle$ and $|V\rangle$ represent the horizontally and the vertically polarized single photon state, respectively. A phase-shift channel transforms the states as $|H\rangle \rightarrow e^{-i\phi}|H\rangle$ and $|V\rangle \rightarrow e^{i\phi}|V\rangle$. The corresponding transformation matrix is given by $W(1, 1, \phi)$. A photon in the state $\alpha|H\rangle + \beta|V\rangle$ is transformed into $e^{-i\phi}(\alpha|H\rangle + e^{2i\phi}\beta|V\rangle)$ by the phase shift. If the phase shift ϕ varies with time and is unknown, the state is distorted. On the other hand, when the state is encoded into two-photon state $\alpha|HV\rangle + \beta|VH\rangle$ and each photon is considered to be altered by the same phase shift represented by $W(1, 1, \phi)$, the state is unchanged as $\alpha|HV\rangle + \beta|VH\rangle$. Thus the logical qubit is protected in the two-qubit DFS spanned by the basis $\{|HV\rangle, |VH\rangle\}$ against

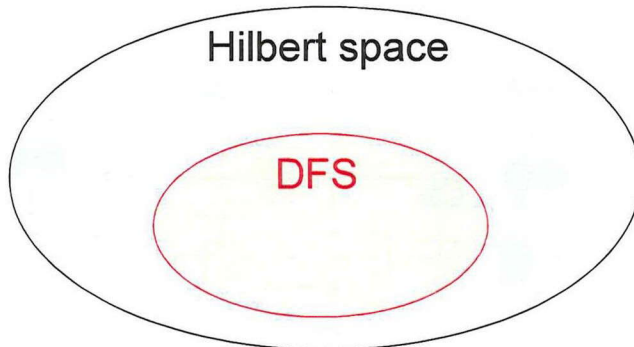


Figure 3.1: Schematic illustration of inclusion relation of Hilbert space and decoherence-free subspace

the collective phase noise. It is well known that the noise in the optical fiber is mainly caused by the fluctuation of the birefringence, which varies slowly with time. Thus the DFS scheme is useful for quantum communication over optical fibers.

In this section, we deal with two types of channels; one is a collective phase noise channel and the other is a general collective noise channel. The transformation matrix for each photon through the collective phase noise channel is written as $W(\gamma_s, \gamma_f, \phi)$, which includes phase shift and polarization dependent losses. In the case of the general collective noise channel, the transformation matrix is expressed by M . We assume the relation (2.73) for transformation matrices of those channels. Since the optical fibers are known to be reciprocal media, such an assumption is valid in optical fiber communications.

In the following subsections, we introduce a protocol that employs one collective phase noise channel and one that employs two general collective noise channels [38, 44]. In all schemes described in this section, we assume that the fluctuations in the channels are so slow that the transformation matrices do not vary with time.

3.2 Single-qubit distribution protocol over collective phase noise

A simple realization of the single-qubit distribution over collective phase noise based on linear optical elements has been proposed in [38]. The procedure of the scheme is as follows: the sender Alice is given a signal photon S in $\alpha|H_S\rangle + \beta|V_S\rangle$ and prepares a reference photon R in a fixed state $|D_R\rangle = \frac{1}{\sqrt{2}}(|H_R\rangle + |V_R\rangle)$, where the subscripts inside $|\cdot\rangle$ represent signal and reference. The time difference between the reference photon and the signal photon are separated in time by Δt as shown

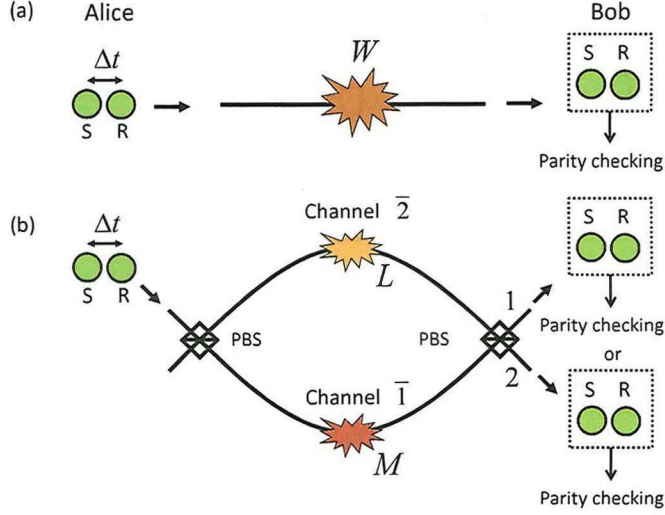


Figure 3.2: Schematic diagram of a single qubit distribution using DFS against (a) a collective phase noise channel and (b) two general collective noise channels. Alice is given the signal photon S and the reference photon R in the fixed state $|D\rangle$. The time difference between the signal and the reference photon is Δt . In the diagram (b), two photons are split into channel $\bar{1}$ and channel $\bar{2}$ by a PBS. The events where two photons appear together in either port 1 or port 2 are selected for the extraction of the state protected by DFS.

in Fig. 3.2(a). After the transmission of the two photons through the channel, the state is described as

$$\frac{1}{\sqrt{2}}[\gamma_s \gamma_f (\alpha |V_R H_S\rangle + \beta |H_R V_S\rangle) + \alpha \gamma_s^2 e^{-2i\phi} |H_R H_S\rangle + \beta \gamma_f^2 e^{2i\phi} |V_R V_S\rangle]. \quad (3.1)$$

The state $\alpha |V_R H_S\rangle + \beta |H_R V_S\rangle$ is in the two-qubit DFS and is invariant under the collective phase noise. The projection of the state (3.1) onto $\alpha |V_R H_S\rangle + \beta |H_R V_S\rangle$ and the decoding of the state to the initial signal state are performed by linear optical parity checking described in Fig. 3.3.

Parity checking measurement

As shown in Fig. 3.3, the linear optical circuits for parity checking aims at the extraction of the state $\alpha |V_R H_S\rangle + \beta |H_R V_S\rangle$ followed by decoding to $\alpha |H_S\rangle + \beta |V_S\rangle$, which works as follows [54, 55, 56]:

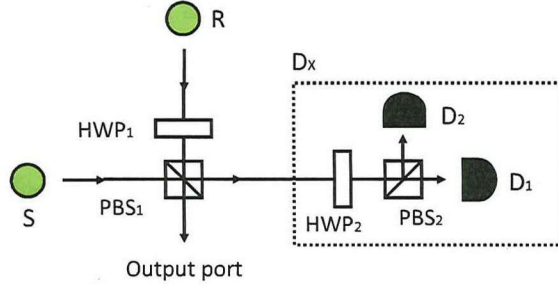


Figure 3.3: Linear optical implementation of the parity checking and decoding. Half wave plates HWP_1 and HWP_2 are rotated by $\pi/4$ and $\pi/8$ from the horizontal axis, respectively. The apparatus D_X surrounded by the dotted box, which includes the photon detector D_1 and D_2 , is used for the projection measurement on the basis $\{|D\rangle, |\bar{D}\rangle\}$. The time difference Δt between the signal and reference photons is compensated in advance by using an optical delay line not shown in the figure.

First one transforms the polarization of the reference photon R as $|H_R\rangle \rightarrow |V_R\rangle$ and $|V_R\rangle \rightarrow |H_R\rangle$ by HWP_1 , and followed by sending the photon R to one port of PBS_1 and the photon S to the other port. The apparatus D_X , which consists of HWP_2 rotated by $\pi/8$, PBS_2 , and photon detectors D_1 and D_2 , measures the incoming photons. The photon detection at D_1 and D_2 correspond to the projection onto the state $|D\rangle$ and $|\bar{D}\rangle$, respectively, when D_X receives a single photon. In the case where the input state is $\alpha|V_R H_S\rangle + \beta|H_R V_S\rangle$, the state just after the PBS_1 is $\alpha|HH\rangle + \beta|VV\rangle$. When the photon detection at D_1 and D_2 occur, the state in the output port becomes $\alpha|H\rangle + \beta|V\rangle$ and $\alpha|H\rangle - \beta|V\rangle$, respectively. Performing the phase shift π only in the case of the photon detection at D_2 , we obtain state $\alpha|H\rangle + \beta|V\rangle$, identical to the initial state. On the other hand, when the input state is in the subspace spanned by $\{|H_R H_S\rangle, |V_R V_S\rangle\}$, two photons leave PBS_1 together from one of the ports, which leads to two- or zero- photon detection in D_X . Thus we can perform the parity checking by linear optics and photon detection. While the photon loss and inefficiency of the detectors leads to the unexpected vacuum in output port, such events can be eliminated by the postselection of the events where the output port is not in the vacuum.

We should also mention that if one or both of the input modes include two or more photons, the scheme in Fig. 3.3 results in errors that are not eliminated by the postselection. In such cases, a single photon detection by the apparatus D_X may leave a single photon in the output port, but

its polarization state will be different from the one intended in the parity checking scheme. In chapters 4 and 5, we discuss protocols using a weak coherent light pulse as the reference, in which case consideration on the rate of such erroneous events is necessary.

Robustness against path-length mismatches between two channels

Here we discuss the robustness of the scheme against path-length mismatches [44]. We neglect the polarization dependent photon losses, since the discussion is focused on the robustness against the path-length difference of two channels. The initial state is described as

$$|D_R\rangle \otimes (\alpha|H_S\rangle_{\Delta t_A} + \beta|V_S\rangle_{\Delta t_A}), \quad (3.2)$$

where Δt_A represent the time delay of the signal photon. We assume Δt_A is much smaller than the correlation time of the fluctuation. The time delay of V -polarized photon for H -polarized photon is represented as τ , and the state of the photons arriving at Bob's side is written as

$$\begin{aligned} & \frac{1}{2}[\alpha e^{-2i\phi}|H_R\rangle|H_S\rangle_{\Delta t_A} + \beta e^{2i\phi}|V_R\rangle_{\tau}|V_S\rangle_{\Delta t_A+\tau} \\ & + (\alpha|V_R\rangle_{\tau}|H_S\rangle_{\Delta t_A} + \beta|H_R\rangle|V_S\rangle_{\Delta t_A+\tau})]. \end{aligned} \quad (3.3)$$

The extraction of the signal state from (3.3) can be performed in the following way. Two photons are split into long path (\bar{L}) and short path (\bar{S}) by BS_B , then mixed by PBS_p again. The remaining procedures are the same as discussed in the previous section. Here we only consider the successful case where the signal photon passes through \bar{S} and the ancillary photon passes through \bar{L} . This happens with the probability 1/4 when two photons arrive at the PBS_p at the same time. In this case, the state just before the PBS_p can be written as

$$\begin{aligned} & \alpha e^{-2i\phi}|V\rangle_{\Delta t_B}^{\bar{L}}|H\rangle_{\Delta t_A}^{\bar{S}} + \beta e^{2i\phi}|H\rangle_{\tau+\Delta t_B}^{\bar{L}}|V\rangle_{\Delta t_A+\tau}^{\bar{S}} \\ & + (\alpha|H\rangle_{\tau+\Delta t_B}^{\bar{L}}|H\rangle_{\Delta t_A}^{\bar{S}} + \beta|V\rangle_{\Delta t_B}^{\bar{L}}|V\rangle_{\Delta t_A+\tau}^{\bar{S}}), \end{aligned} \quad (3.4)$$

where subscripts represent the spacial modes. If one photon is found in each output mode of X and Y , the state just after the PBS_p is $\alpha|H\rangle_{\tau+\Delta t_B}^Y|H\rangle_{\Delta t_A}^X + \beta|V\rangle_{\Delta t_B}^X|V\rangle_{\Delta t_A+\tau}^Y$ ¹. Let us consider the case where $\Delta t_A = \Delta t_B = \Delta \bar{t}$. When the detector D_X finds one photon, the state in mode Y is projected onto the state $\alpha|H\rangle_{\tau+\Delta \bar{t}}^Y + \beta|V\rangle_{\Delta \bar{t}+\tau}^Y$. The important point is that the time delay τ affects only the arrival time but not the fidelity of the output state. This shows the robustness of this scheme against the path-length mismatches.

¹This expression can be also written $\alpha|H\rangle_{\Delta t_A}^X|H\rangle_{\tau+\Delta t_B}^Y + \beta|V\rangle_{\Delta t_B}^X|V\rangle_{\Delta t_A+\tau}^Y$.

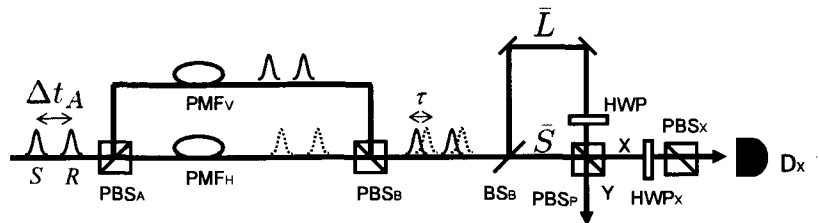


Figure 3.4: Schematic diagram of the single qubit distribution. In spite of the path-length mismatches of two transmission lines, this scheme works well. The detail is discussed in the text.

3.3 Single-qubit distribution protocol over general collective noise

The scheme in the previous subsection protects a qubit against a collective phase noise channel, but a small modification achieves the protection of the signal state against the general collective noise channels, if we are allowed to use two of such channels as in Fig. 3.2(b) [38]. The two channels are combined by a PBS at the sender and by another PBS at the receiver. Let the transformation matrices of the channels $\bar{1}$ and $\bar{2}$ be

$$M = \begin{pmatrix} m_1 & m_2 \\ m_3 & m_4 \end{pmatrix} \text{ and } L = \begin{pmatrix} l_1 & l_2 \\ l_3 & l_4 \end{pmatrix}, \quad (3.5)$$

respectively. The signal (reference) photon in state $|H_{S(R)}\rangle$ and $|V_{S(R)}\rangle$ is transformed as $|H_{S(R)}\rangle \rightarrow m_1|H_{S(R)}\rangle + m_3|V_{S(R)}\rangle$ and $|V_{S(R)}\rangle \rightarrow l_2|H_{S(R)}\rangle + l_4|V_{S(R)}\rangle$. After the photons S and R pass through the channels $\bar{1}$ and $\bar{2}$, the state is written as

$$\begin{aligned} & \frac{1}{\sqrt{2}} [\alpha m_1^2 |H_R H_S\rangle_{11} + m_1 m_3 |H_R V_S\rangle_{12} + m_3 m_1 |V_R H_S\rangle_{21} + m_3^2 |V_R V_S\rangle_{22}) \\ & + \beta (m_1 l_2 |H_R H_S\rangle_{12} + m_1 l_4 |H_R V_S\rangle_{11} + m_3 l_2 |V_R H_S\rangle_{22} + m_3 l_4 |V_R V_S\rangle_{21}) \\ & + \alpha (l_2 m_1 |H_R H_S\rangle_{21} + l_2 m_3 |H_R V_S\rangle_{22} + l_4 m_1 |V_R H_S\rangle_{11} + l_4 m_3 |V_R V_S\rangle_{12}) \\ & + \beta (l_2^2 |H_R H_S\rangle_{22} + l_2 l_4 |H_R V_S\rangle_{21} + l_4 l_2 |V_R H_S\rangle_{12} + l_4^2 |V_R V_S\rangle_{11})]. \end{aligned} \quad (3.6)$$

The subscripts outside of $|\cdot\rangle$ represent the output port numbers. When two photons appear in port 1, the state is written as $\frac{1}{\sqrt{2}} [m_1^2 \alpha |H_R H_S\rangle_{11} + m_1 l_4 (\beta |H_R V_S\rangle_{11} + \alpha |V_R H_S\rangle_{11}) + l_4^2 \beta |V_R V_S\rangle_{11}]$. The state $\frac{1}{\sqrt{2}} m_1 l_4 (\beta |H_R V_S\rangle_{11} + \alpha |V_R H_S\rangle_{11})$ is invariant under the collective noise. Similarly to the

previous scheme, the parity checking shown in Fig. 3.3 achieves the extraction of the signal state $\alpha|H\rangle + \beta|V\rangle$. When the photons R and S appear at port 2, the state is written as $\frac{1}{\sqrt{2}}[m_3^2\alpha|V_RV_S\rangle_{22} + m_3l_2(\beta|V_RH_S\rangle_{22} + \alpha|H_RV_S\rangle_{22}) + l_2^2\beta|H_RH_S\rangle_{22}]$. The state $\frac{1}{\sqrt{2}}m_3l_2(\beta|V_RH_S\rangle_{22} + \alpha|H_RV_S\rangle_{22})$ is again invariant under the general collective noise and is decoded into the signal state. As shown in the above discussion, two channels together with PBSs enable us to reject the polarization rotation errors and to extract the signal state.

The success probability of the case where two photons emerge at port 1 is given by $|m_1|^2|l_4|^2/2$, but this value is sensitive to a small change in birefringence of the fiber. By inserting random unitary operations at both ends of channel $\bar{1}$ and channel $\bar{2}$, we can make the success probability to be a more stable quantity of $T_1T_2/4$, where $T_1 \equiv \text{Tr}(M^\dagger M)/2$ and $T_2 \equiv \text{Tr}(L^\dagger L)/2$ are the polarization-averaged transmission of the channels. The success probability for two photons leaving port 2 is also given by $T_1T_2/4$, leading to the overall success probability $T_1T_2/2$.

The schemes described in this chapter are able to protect arbitrary *unknown* states of a qubit, and hence they are also able to protect any correlation that is initially formed between the input qubit and other systems. Those schemes can thus be used for distributing a maximally entangled state of a qubit pair through channels with collective noises. In the following chapters, we discuss protocols solely intended for such a distribution of a maximally entangled state, with an added benefit of an improved scaling of the efficiency over the channel transmission.

3.4 4-qubit DFS protocol

In previous sections, we have considered single-qubit distribution schemes with the help of an ancillary qubit. The ancillary qubit is used to fight against the channel noise by composing the decoherence-free subspace with the signal qubit. These protocols which we have introduced are based on a two-qubit DFS scheme.

In this section, we introduce faithful qubit distribution scheme which is base on a four-qubit DFS. The idea which we introduce here is to send the logical qubit, which is immune to the channel noise [40, 57]. First, we introduce the robustness of the singlet state $|\psi^-\rangle = \frac{1}{\sqrt{2}}(|01\rangle - |10\rangle)$ against the collective unitary as follows:

$$(U \otimes U)|\psi^-\rangle = e^{i\theta}|\psi^-\rangle, \quad (3.7)$$

where $e^{i\theta}$ is a global phase. We define a logical zero qubit as $|0\rangle_L$ and a logical one qubit as $|1\rangle_L$ so that the inner product between $|0\rangle_L$ and $|1\rangle_L$ is orthogonal and written as follows (See also Fig. 3.5

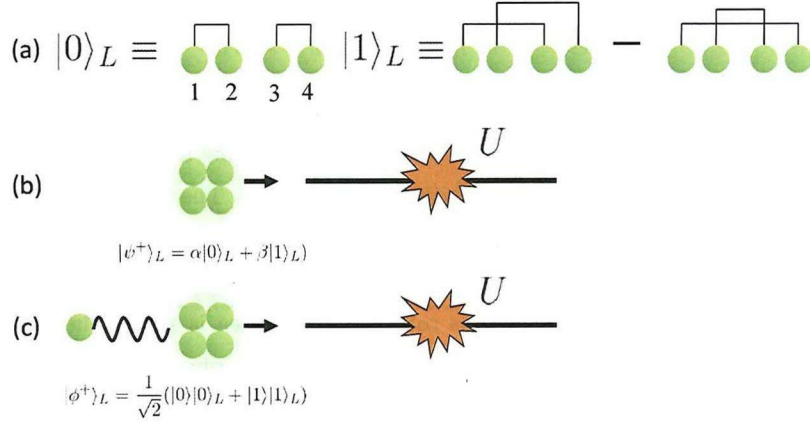


Figure 3.5: (a) Illustration of the logical qubits. The connected qubits represent the singlet state. (b) The distribution of the single state using logical qubit and (c) the entangled state. Robustness against a general collective noise of the singlet state is used in these schemes.

(a.):

$$\begin{aligned} |0\rangle_L &= |\psi^-\rangle_{12}|\psi^-\rangle_{34} \\ &= \frac{1}{2}(|0101\rangle - |0110\rangle - |1001\rangle + |1010\rangle) \end{aligned} \quad (3.8)$$

and

$$\begin{aligned} |1\rangle_L &= |\psi^-\rangle_{13}|\psi^-\rangle_{24} - |\psi^-\rangle_{14}|\psi^-\rangle_{23} \\ &= \frac{1}{2\sqrt{3}}(2|0011\rangle - |0101\rangle - |0110\rangle - |1001\rangle - |1010\rangle + 2|1100\rangle). \end{aligned} \quad (3.9)$$

Both logical qubits $|0\rangle_L$ and $|1\rangle_L$ are the superposition of the singlet states and robust against a general type of the channel noise, i.e., the following relation holds:

$$U^{\otimes 4}|0\rangle_L = e^{i\theta}|0\rangle_L \quad (3.10)$$

and

$$U^{\otimes 4}|1\rangle_L = e^{i\theta}|1\rangle_L. \quad (3.11)$$

Using this property, Alice prepares an arbitrary state

$$|\psi\rangle_L = \alpha|0\rangle_L + \beta|1\rangle_L \quad (3.12)$$

and sends it to Bob. The illustration of the scheme is shown in Fig. 3.5 (b). After receiving four photons, the state is described as

$$|\psi\rangle_L \xrightarrow{U^{\otimes 4}} |\psi'\rangle_L = e^{i\theta}(\alpha|0\rangle_L + \beta|1\rangle_L). \quad (3.13)$$

After decoding, Bob successfully obtains a single qubit state $|\psi\rangle = \alpha|0\rangle + \beta|1\rangle$.

This scheme is generalized to entanglement distribution scheme as shown in Fig. 3.5 (c). Alice prepares a logical entangled state $|\phi^+\rangle_L = \frac{1}{\sqrt{2}}(|0\rangle|0\rangle_L + |1\rangle|1\rangle_L)$. The qubits which are sent to Bob is composed of the logical qubits. After receiving the logical qubits, Bob decodes back to the normal entangled pair $|\phi^+\rangle = \frac{1}{\sqrt{2}}(|0\rangle|0\rangle + |1\rangle|1\rangle)$.

This entanglement distribution scheme is robust and the idea is simple, however, distribution rate is quite serious, since the signal qubit is composed of four photons. This means that if the transmittance of the channel is $T = 0.01$, the success probability of this scheme is proportional to 10^{-8} . The distribution protocol which realize both the immunity again the channel noise and high performance whose success probability is proportional to T is introduced later in chapter 5.

Chapter 4

Entanglement distribution protocol with counter-propagating photons

A serious drawback of the photonic DFS schemes including the previously introduced schemes is the inefficiency caused by the photon loss in optical fibers. When the transmittance of the channel is T and a two-qubit DFS scheme is performed, the success probability for sending a qubit state is proportional to T^2 . In order to overcome the inefficiency, a two-qubit DFS scheme based on a backward-propagating weak coherent light pulse over the collective phase noise channel, whose efficiency is proportional to T , has been proposed and demonstrated in Ref. [46]. In this chapter, we introduce the working principle of the scheme in the case where the backward-propagating light is initially a single photon, and then we show that the efficiency is improved by using a coherent light pulse instead of the single photon.

4.1 Equivalent operation on entangled states

Before the explanation of the scheme, we first derive an important property of entangled state, which is used within the scheme. We introduce d -dimensional bipartite maximally entangled state $|\phi_d^+\rangle_{AB} \equiv \sum_{i=1}^d |i\rangle_A |i\rangle_B$. An important property of maximally entangled state is

$$(I_A \otimes M_B)|\phi_d\rangle_{AB} = (M_A^T \otimes I_B)|\phi_d\rangle_{AB}, \quad (4.1)$$

where M is an operator and M^T is the transpose of the operator M . This is because, for all j and k ,

$$\begin{aligned}\langle j|_A|k\rangle_B(I_A \otimes M_B)\langle\phi_d|_{AB} &= \langle k|_B M_B|j\rangle_B/\sqrt{d} \\ &= \langle k|_A M_A^T|j\rangle_A/\sqrt{d} \\ &= \langle j|_A|k\rangle_B(M_A^T \otimes I_B)\langle\phi_d|_{AB}\end{aligned}\quad (4.2)$$

is satisfied. From Eq. (4.1), a bipartite two-qubit system satisfies

$$(I_A \otimes U_B)|\phi^+\rangle_{AB} = (U_A^T \otimes I_B)|\phi^+\rangle_{AB}, \quad (4.3)$$

where U is a unitary operator acting on a subsystem. Since the single state $|\psi^-\rangle$ is expressed as $|\psi^-\rangle_{AB} = (iY_A \otimes I_B)|\phi^+\rangle_{AB}$, then we obtain

$$\begin{aligned}(I_A \otimes U_B)|\psi^-\rangle_{AB} &= (I_A \otimes U_B)(iY_A \otimes I_B)|\phi^+\rangle_{AB} \\ &= (iY_A U_A^T \otimes I_B)|\phi^+\rangle_{AB} \\ &= (iY_A U_A^T (iY_A)^\dagger \otimes I_B)|\psi^-\rangle_{AB} \\ &= (U_A^\dagger \otimes I_B)|\psi^-\rangle_{AB}.\end{aligned}\quad (4.4)$$

Eq. (4.4) means that a unitary operation U_B on the subsystem B is equivalent to a unitary operation U_A^\dagger that of on A . In a similar manner, the properties of another Bell state is shown in the following table:

Bell state	equivalent operation on A
$ \phi^+\rangle_{AB}$	U_A^T
$ \phi^-\rangle = (I_A \otimes Z_B) \phi^+\rangle_{AB}$	$Z_A U_A^T Z_A$
$ \psi^+\rangle = (I_A \otimes X_B) \phi^+\rangle_{AB}$	$X_A U_A^T X_A$
$ \psi^-\rangle = (I_A \otimes iY_B) \phi^+\rangle_{AB}$	$Y_A U_A^T Y_A$

Table 4.1: The relationship between the local operation on B and its equivalent operation on A .

From Eq. (4.1), when a local unitary operation U is diagonal as $U = u_{11}|0\rangle\langle 0| + u_{22}|1\rangle\langle 1|$, we obtain

$$(I_A \otimes U_B)|\phi^+\rangle_{AB} = (U_A \otimes I_B)|\phi^+\rangle_{AB}, \quad (4.5)$$

which means that we can regard the operation U on B as that of on A .

4.2 Counter-propagating protocol

A two-qubit DFS scheme which is discussed in Chapter 3, both the signal photon and the ancillary photon are sent from Alice to Bob. We now suppose that Bob, instead of Alice, sends a reference photon R in the state $|D_R\rangle = \frac{1}{\sqrt{2}}(|H_R\rangle + |V_R\rangle)$ to Alice as shown in Fig. 4.1. Alice prepares photons A and S in an entangled state $|\phi_{AS}^+\rangle = \frac{1}{\sqrt{2}}(|H_A H_S\rangle + |V_A V_S\rangle)$, and sends the signal photon S to Bob through the channel. The transformation matrix $W(\gamma_s, \gamma_f, \phi)$ is used again for the collective phase noise channel. The transformation matrix for the backward propagation is the same as $W(\gamma_s, \gamma_f, \phi)$ ¹. After transmission, two photons A and R are at Alice's side and the signal photon S is at Bob's side. The state of the three photons are described as

$$\begin{aligned} & \frac{1}{2}[\gamma_s \gamma_f (|H_R V_S\rangle |V_A\rangle + |V_R H_S\rangle |H_A\rangle) \\ & + \gamma_s^2 e^{-2i\phi} |H_R H_S\rangle |H_A\rangle + \gamma_f^2 e^{2i\phi} |V_R V_S\rangle |V_A\rangle]. \end{aligned} \quad (4.6)$$

Here we have used a property that when two qubits A and S are in the entangled state $|\phi_{AS}^+\rangle$, a phase shift on qubit S is equivalent to the same amount of phase shift on qubit A , which is discussed in the Sec. 4.1. Thus the net effect is the same as if photons A and R had passed through the collective phase noise channel as shown in Fig. 4.2. Thanks to this property, in spite of the counter-propagation of the ancillary photon, it is possible to construct a two-qubit DFS. After performing the parity checking on qubit A and R at Alice's side, they obtain the entangled state over the collective phase noise channel.

4.3 Boosting up the efficiency using WCP

The efficiency of the protocol using a single photon as the reference photon R is obviously $O(T^2)$. The modification to improve the efficiency is done as follows: Bob sends a coherent light pulse, instead of a single photon, to Alice. Let μ be the average photon number of the coherent pulse received by Alice, after passing through the channel with transmission T . The probabilities of one photon and two or more photons are contained in the coherent light pulse at Alice's side are $P_1 = O(\mu)$ and $P_m = O(\mu^2)$, respectively. In this protocol, the successful events accepted by the linear optical parity checking consists of two cases; (i) one photon is in mode A and one photon is in the reference mode R , and (ii) two or more photons are in the reference mode R . Since mode A always has a single photon, the probability of the case (i) is $O(\mu)$ and that of the case (ii) is $O(\mu^2)$. As described in the previous chapter, the case (ii) causes the degradation of the fidelity. Thus, $O(\mu) \gg O(\mu^2)$, which leads to the condition $\mu \ll 1$, should be satisfied for high fidelity entanglement distribution.

¹Of course, this can be confirmed using the Eq. (2.73). If you do not use this equation, it can be understood from the fact that $W(\gamma_s, \gamma_f, \phi)$ is diagonal.

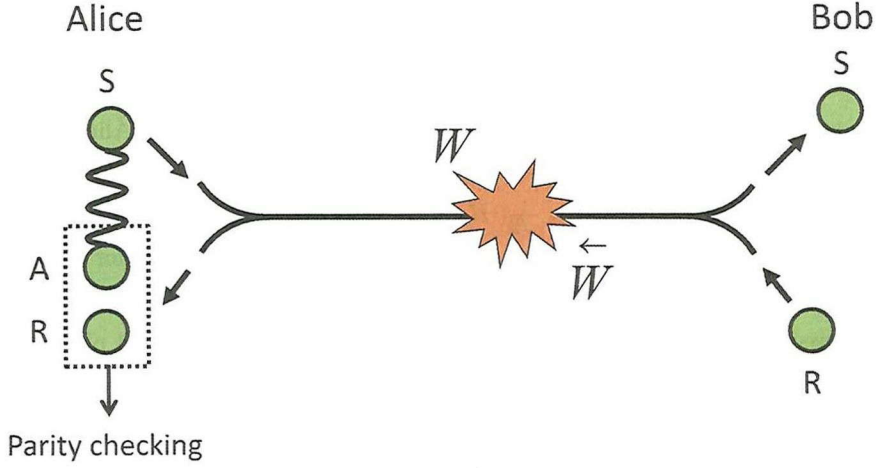


Figure 4.1: Schematic diagram of entanglement distribution scheme using the backward-propagating reference photon. Alice prepares the entangled photon pair $|\phi_{AS}^+\rangle$ and sends the photon S to Bob. On the other hand, Bob prepares the reference photon R and sends it to Alice. After receiving the photon R , Alice performs parity checking on photons A and R to extract the DFS and decodes back to the entangled state $|\phi^+\rangle$. In order to boost up the efficiency, Bob uses a weak coherent light pulse, in stead of a single photon, as the reference light.

Although the condition $\mu \ll 1$ must be satisfied, μ can be chosen independent of the channel transmittance T . Thus the overall success probability, which is $O(\mu T)$, is proportional to T . Note that there is a trade-off between the achievable efficiency and fidelity of this protocol with respect to the value of μ . The advantage of the scheme in the case of low T regime has been experimentally demonstrated in Ref. [46].

4.4 Discussion

One might wonder why we cannot apply the same technique to the forward propagation protocols in Chap. 3 to improve the efficiency. However, as long as we use the linear optical parity checking in Fig. 3.3 at Bob's side, we do not obtain the efficiency $O(T)$ by using WCP as the reference photon. Suppose that Bob receives a WCP with mean photon number μ . The probability that either of mode S and mode R has exactly one photon, corresponding to the case (i) above, is $O(\mu T)$ since the signal photon S must have survived the lossy channel. Therefore $O(\mu T) \gg O(\mu^2)$, which leads to $\mu \ll T$, should be satisfied for a high fidelity. This limits the overall success probability to be $O(T^2)$.

Intuitively, this can be considered as follows: Bob is not able to distinguish the expected event

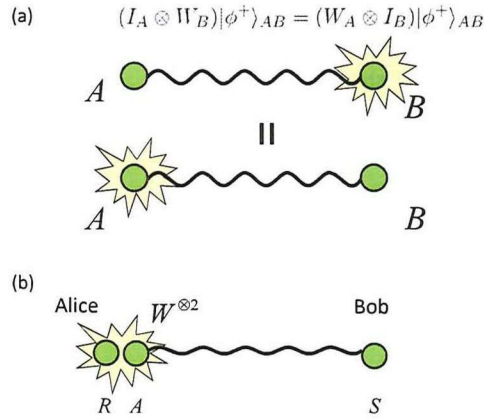


Figure 4.2: (a) The equivalence of the channel noise on signal photon and Alice’s photon. (a) The illustration shows that the noise on the signal photon, which forms an entangled photon pair with Alice’s photon, is equal to that of on Alice’s photon. (b) Using the property of (a), we can regard that both the ancillary photon and Alice’s photon are affected by the channel noise.

and the unexpected event. That is to say, when he receives the two photons from Alice, he can not discriminate the event where one photo is the signal photon and the other is the ancillary photon from both photons are the ancillary photons. This makes them no longer possible to share entangled state with success probability to be proportional to T , so counter propagation of the ancillary photon is indispensable in this scheme.

4.5 Summary

In this chapter, we have considered the entanglement distribution scheme which can be realized with success probability to be proportional to T . In order to achieve this, a WCP is used as ancillary photon instead of the single photon. Sending the ancillary photon from Bob to Alice is also important. Sending the signal photon together with the ancillary photon was common-sense approach, since it is easy to understand that these qubits experience the same collective noise. On the other hand, it is not clear whether counter-propagating two-qubit DFS scheme works out or not. Thanks to the important relation Eq. (4.5), the counter-propagating two-qubit DFS become possible.

This scheme is robust against phase noise of the channel, however, this scheme does not suppose a general type of the channel noise. In fact, the polarization maintaining optical fiber is used to demonstrate this scheme. Next chapter we propose a new entanglement distribution protocol which is robust against a general type of the channel noise.

Chapter 5

Entanglement distribution protocol over general collective noise with counter-propagating photons

In this chapter, we newly propose an extended scheme that applies the counter propagation protocol to the two-channel scheme introduced in Sec. 3.3, in order to boost up the efficiency of the two-qubit DFS scheme against the general collective noise channels. The key ingredient in the scheme is the relation (2.73), which is believed to be satisfied in optical fibers. In the same manner as in the previous chapter, we first introduce the working principle using a single photon as an ancillary photon.

5.1 Working principle of the proposed protocol

As shown in Fig. 5.1, Alice prepares the entangled state $|\phi_{AS}^+\rangle$ and sends the signal photon S to Bob. Bob prepares the reference photon R in the state $|D_R\rangle$ and sends it to Alice. The signal photon S is split into two spacial modes by a PBS. The reference photon R is also split into two spacial modes by a PBS. The state just before the signal and reference photons entering channel $\bar{1}$ and $\bar{2}$ is

$$\begin{aligned} & \frac{1}{2}(|H_R H_S\rangle_{\bar{1}\bar{1}}|H_A\rangle + |H_R V_S\rangle_{\bar{1}\bar{2}}|V_A\rangle \\ & + |V_R H_S\rangle_{\bar{2}\bar{1}}|H_A\rangle + |V_R V_S\rangle_{\bar{2}\bar{2}}|V_A\rangle). \end{aligned} \quad (5.1)$$

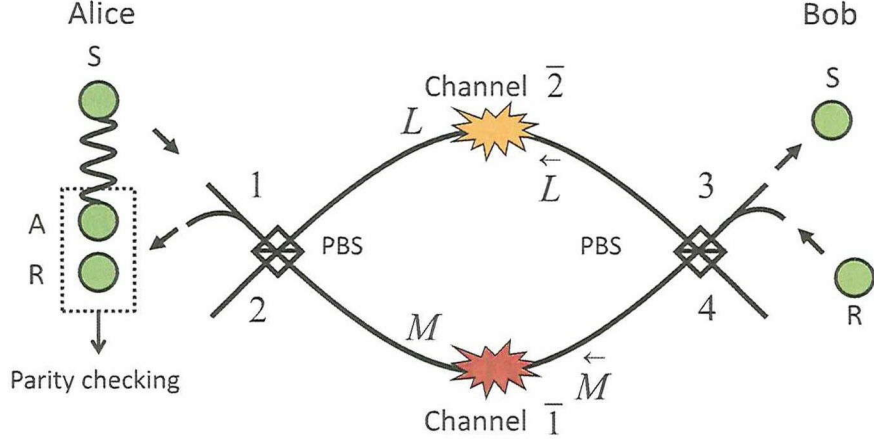


Figure 5.1: Schematic diagram of the proposed entanglement distribution protocol. Only when photon R appears in port 1 and photon S appears in port 3, the state protected by DFS is extracted. Our protocol is robust against a general type of the channel noise and the distribution rate is proportional to T .

Suppose that the transformation matrices of channels $\bar{1}$ and $\bar{2}$ are

$$M = \begin{pmatrix} m_1 & m_2 \\ m_3 & m_4 \end{pmatrix} \text{ and } L = \begin{pmatrix} l_1 & l_2 \\ l_3 & l_4 \end{pmatrix}, \quad (5.2)$$

which are the same as in Eq. (3.5). As discussed in Sec. 2.4, the corresponding transformation matrices for the backward propagation are $\overleftarrow{M} = ZM^T Z$ and $\overleftarrow{L} = ZL^T Z$, which is written as

$$\overleftarrow{M} = \begin{pmatrix} m_1 & -m_3 \\ -m_2 & m_4 \end{pmatrix} \text{ and } \overleftarrow{L} = \begin{pmatrix} l_1 & -l_3 \\ -l_2 & l_4 \end{pmatrix}, \quad (5.3)$$

respectively. After the photons pass through the channel $\bar{1}$ and $\bar{2}$, signal photon is transformed as $|H_S\rangle \rightarrow m_1|H_S\rangle + m_3|V_S\rangle$ and $|V_S\rangle \rightarrow l_2|H_S\rangle + l_4|V_S\rangle$, while the ancillary photon is transformed as $|H_R\rangle \rightarrow m_1|H_R\rangle - m_2|V_R\rangle$ and $|V_R\rangle \rightarrow -l_3|H_R\rangle + l_4|V_R\rangle$, and the state is written as

$$\begin{aligned} & \frac{1}{2} [(m_1|H_R\rangle_{\bar{1}} - m_2|V_R\rangle_{\bar{1}})(m_1|H_S\rangle_{\bar{1}} + m_3|V_S\rangle_{\bar{1}})|H_A\rangle \\ & + (m_1|H_R\rangle_{\bar{1}} - m_2|V_R\rangle_{\bar{1}})(l_2|H_S\rangle_{\bar{2}} + l_4|V_S\rangle_{\bar{2}})|V_A\rangle \\ & + (-l_3|H_R\rangle_{\bar{2}} + l_4|V_R\rangle_{\bar{2}})(m_1|H_S\rangle_{\bar{1}} + m_3|V_S\rangle_{\bar{1}})|H_A\rangle \\ & + (-l_3|H_R\rangle_{\bar{2}} + l_4|V_R\rangle_{\bar{2}})(l_2|H_S\rangle_{\bar{2}} + l_4|V_S\rangle_{\bar{2}})|V_A\rangle]. \end{aligned} \quad (5.4)$$

After that, both photons pass through the PBSs. The state then becomes

$$\begin{aligned}
& \frac{1}{2}[(m_1^2|H_R H_S\rangle_{13} + m_1 m_3|H_R V_S\rangle_{14} - m_2 m_1|V_R H_S\rangle_{23} - m_2 m_3|V_R V_S\rangle_{24})|H_A\rangle \\
& + (m_1 l_2|H_R H_S\rangle_{14} + m_1 l_4|H_R V_S\rangle_{13} - m_2 l_2|V_R H_S\rangle_{24} - m_2 l_4|V_R V_S\rangle_{23})|V_A\rangle \\
& + (-l_3 m_1|H_R H_S\rangle_{23} - l_3 m_3|H_R V_S\rangle_{24} + l_4 m_1|V_R H_S\rangle_{13} + l_4 m_3|V_R V_S\rangle_{14})|H_A\rangle \\
& + (-l_3 l_2|H_R H_S\rangle_{24} - l_3 l_4|H_R V_S\rangle_{23} + l_4 l_2|V_R H_S\rangle_{14} + l_4^2|V_R V_S\rangle_{13})|V_A\rangle]. \quad (5.5)
\end{aligned}$$

After post-selecting the event where the photons R and S appear at port 1 and 3, we obtain the state

$$\begin{aligned}
& \frac{1}{2}[m_1^2|H_R H_S\rangle_{13}|H_A\rangle + m_1 l_4(|H_R V_S\rangle_{13}|V_A\rangle \\
& + |V_R H_S\rangle_{13}|H_A\rangle) + l_4^2|V_R V_S\rangle_{13}|V_A\rangle]. \quad (5.6)
\end{aligned}$$

Fortunately, a part of the state $\frac{1}{2}m_1 l_4(|H_R V_S\rangle_{13}|V_A\rangle + |V_R H_S\rangle_{13}|H_A\rangle)$ is invariant under the general collective noise. In the same manner as in Chap. 4, Alice can extract the state by using linear optical parity checking in Fig. 3.3. The final state shared between Alice and Bob is the maximally entangled state $|\phi^+\rangle$. As shown Eq. (5.5), unlike the forward propagation protocol shown in Sec. 3.3, the state of the photons appearing in the other ports, 2 and 4, is not protected over the general collective noise channels. By inserting random unitary operations the overall success probability becomes $T_1 T_2/4$, which is half of that in Sec. 3.3 due to the fact that the cases for photons leaving ports 2 and 4 automatically fails. This success probability can then be boosted up by using WCP as the reference light, from $O(T^2)$ to $O(T)$.

In the forward-propagating protocol shown in Fig. 3.2 (b), when both photons appear at port 1, there are two possible trajectories: $H \rightarrow H/\bar{1}$, implying that an H polarized photon enters channel $\bar{1}$ and leaves in H polarization, and $V \rightarrow V/\bar{2}$. If the signal photon has H polarization, it takes the former and the reference photon takes the latter. If the signal photon has V polarization, they just interchanges the trajectories and acquire the same phase shift together. The same argument applies when both photons appear in port 2, with two trajectories $H \rightarrow V/\bar{1}$ and $V \rightarrow H/\bar{2}$. In the backward-propagating protocol presented in this subsection, we have four trajectories instead. When the photons appear at ports 1 and 3, those are $H \rightarrow H/\bar{1}$ and $V \rightarrow V/\bar{2}$ for photon S , and $H \leftarrow H/\bar{1}$ and $V \leftarrow V/\bar{2}$ for photon R , where the trajectories for photon R are the time-reversed versions of those for photon S . As a result, two possible choices of the trajectories of the two photons, shown in Fig. 5.2 (a), acquire the same phase shift from the channels. On the other hand, when the photons appear at ports 2 and 4, the relevant trajectories are $H \rightarrow V/\bar{1}$ and $V \rightarrow H/\bar{2}$ for photon S , and $H \leftarrow V/\bar{2}$ and $V \leftarrow H/\bar{1}$ for photon R , among which no pair are in the time-reversal relation. Hence no state is protected in this case.

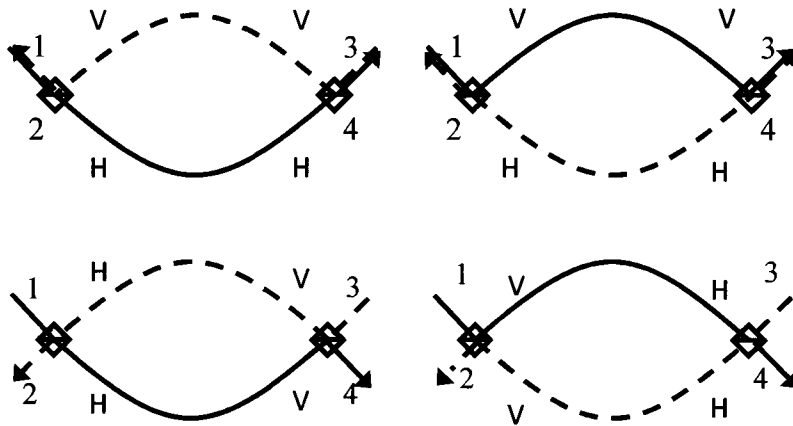


Figure 5.2: Sketch of the trajectories when two photons appear in (a) port 1 and 3 or (b) port 2 and 4. The solid arrows and the dotted arrows show the trajectories of the signal and the reference photon, respectively.

Several remarks are in order for the experimental realization of the proposed scheme using WCP. In practice, polarization independent optical circulator with high efficiency is hard to obtain. However, such a device is not required when we use WCP as the reference. In that case, we may replace the optical circulator by small reflectance mirrors, which transmit the signal photon with transmittance close to unity and reflect the reference photons. The low reflectance can simply be compensated by increasing the initial amplitude of the WCP. The optical path length mismatch between the two channels needs to be adjusted within the coherence length of the photons, which is typically far longer than the wavelength of the photons. Similarly to the experiment in Ref. [46], the experimental demonstration can be done by using the entangled photon source based on parametric down conversion, linear optical elements and photon detectors. The scheme is also robust against the fluctuations in the optical circuits used for parity checking due to the two-photon interference.

5.2 Time-bin protocol

We now consider an alternative scheme which uses the time-bin encoding, which is used, for example, time-bin encoding BB84 protocol [58, 59]. We apply this idea to entanglement distribution protocol which is discussed in the previous section. The schematic diagram of this scheme is shown in Fig.

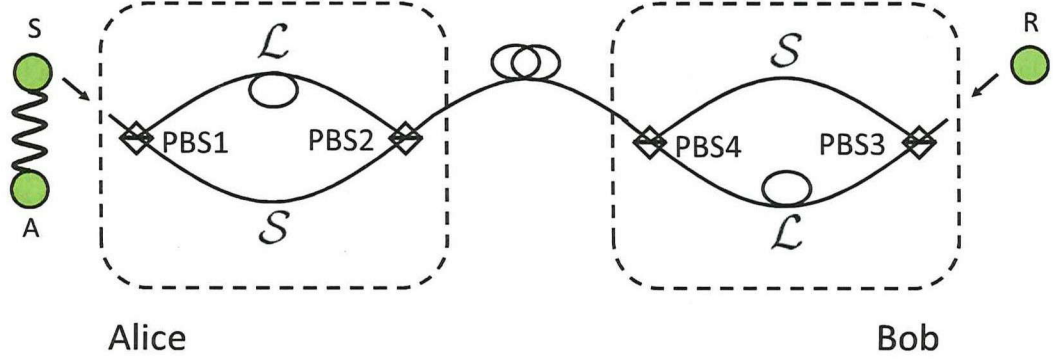


Figure 5.3: Schematic diagram of the entanglement distribution scheme based on the time-bin encoding. Alice and Bob successfully share an entangled state by postselecting the event where both the signal photon and the ancillary photon pass through $\mathcal{L}\mathcal{S}$ or $\mathcal{S}\mathcal{L}$.

5.3. At Alice's side the signal photon S is split into the short path S and the long path \mathcal{L} by PBS1. H polarized photon passes through S and V polarized photon passes through \mathcal{L} . The time difference between H polarized photon and V polarized photon after passing through PBS2 is set to Δt . On the other hand, at Bob's side, the ancillary photon is also split into the short path S and the long path \mathcal{L} . In this time, H polarized photon passes through the long path and V polarized photon passes through the short path. Likewise the time difference between H polarized photon and V polarized photon is set to Δt . After passing through the PBS3 and PBS4 the state is written as

$$\frac{1}{2}(|H_R\rangle_{\mathcal{L}} + |V_R\rangle_{\mathcal{S}})(|H_S\rangle_{\mathcal{S}}|H_A\rangle + |V_S\rangle_{\mathcal{L}}|V_A\rangle). \quad (5.7)$$

The channel noise is represented by M and L for forward propagation and \overleftarrow{M} and \overleftarrow{L} for backward propagation, which are used at (5.2) and (5.3). Through the noisy channel, the signal photon is transformed as $|H_S\rangle \rightarrow m_1|H_S\rangle_{\mathcal{S}} + m_3|V_S\rangle_{\mathcal{S}}$ and $|V_S\rangle \rightarrow m_2|H_S\rangle_{\mathcal{L}} + m_4|V_S\rangle_{\mathcal{L}}$. In the same manner the ancillary photon is transformed as $|H_R\rangle \rightarrow m_1|H_R\rangle_{\mathcal{L}} - m_2|V_R\rangle_{\mathcal{L}}$ and $|V_R\rangle \rightarrow -m_3|H_R\rangle_{\mathcal{S}} + m_4|V_R\rangle_{\mathcal{S}}$. The signal photon enters PBS4 and H polarized photon goes into the long path and V polarized photon goes into the short path. While the ancillary photon enters PBS2 and H polarized photon goes into the short path and V polarized photon goes into the long path. After passing

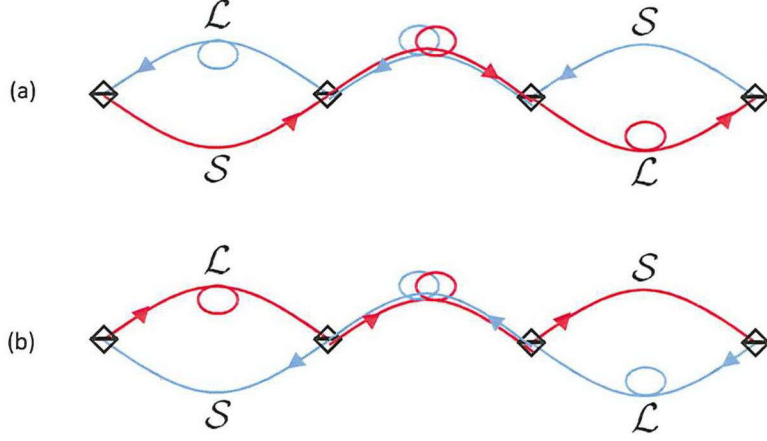


Figure 5.4: The schematic of the trajectory of the success event. The red (blue) line represents the trajectories of the signal (ancillary) photon. (a) The trajectory of the signal photon which pass through $\mathcal{S} \rightarrow \mathcal{L}$ and the ancillary photon which pass through $\mathcal{S} \rightarrow \mathcal{L}$. (b) The trajectory of the signal photon which pass through $\mathcal{L} \rightarrow \mathcal{S}$ and the ancillary photon which pass through $\mathcal{L} \rightarrow \mathcal{S}$.

through PBS1 and PBS3, we obtain

$$\begin{aligned}
& \frac{1}{2} [(m_1^2 |H_R\rangle_{\mathcal{L}\mathcal{S}} |H_S\rangle_{\mathcal{S}\mathcal{L}} + m_1 m_3 |H_R\rangle_{\mathcal{L}\mathcal{S}} |V_S\rangle_{\mathcal{S}\mathcal{S}} - m_2 m_1 |V_R\rangle_{\mathcal{L}\mathcal{L}} |H_S\rangle_{\mathcal{S}\mathcal{L}} - m_2 m_3 |V_R\rangle_{\mathcal{L}\mathcal{L}} |V_S\rangle_{\mathcal{S}\mathcal{S}}) |H\rangle \\
& + (m_1 m_2 |H_R\rangle_{\mathcal{L}\mathcal{S}} |H_S\rangle_{\mathcal{L}\mathcal{L}} + m_1 m_4 |H_R\rangle_{\mathcal{L}\mathcal{S}} |V_S\rangle_{\mathcal{L}\mathcal{S}} - m_2^2 |V_R\rangle_{\mathcal{L}\mathcal{L}} |H_S\rangle_{\mathcal{L}\mathcal{L}} - m_2 m_4 |V_R\rangle_{\mathcal{L}\mathcal{L}} |V_S\rangle_{\mathcal{L}\mathcal{S}}) |V\rangle \\
& + (-m_3 m_1 |H_R\rangle_{\mathcal{S}\mathcal{S}} |H_S\rangle_{\mathcal{S}\mathcal{L}} - m_3^2 |H_R\rangle_{\mathcal{S}\mathcal{S}} |V_S\rangle_{\mathcal{S}\mathcal{S}} + m_4 m_1 |V_R\rangle_{\mathcal{S}\mathcal{L}} |H_S\rangle_{\mathcal{S}\mathcal{L}} + m_4 m_3 |V_R\rangle_{\mathcal{S}\mathcal{L}} |V_S\rangle_{\mathcal{S}\mathcal{S}}) |H\rangle \\
& + (-m_3 m_2 |H_R\rangle_{\mathcal{S}\mathcal{S}} |H_S\rangle_{\mathcal{L}\mathcal{L}} - m_3 m_4 |H_R\rangle_{\mathcal{S}\mathcal{S}} |V_S\rangle_{\mathcal{L}\mathcal{S}} + m_4 m_2 |V_R\rangle_{\mathcal{S}\mathcal{L}} |H_S\rangle_{\mathcal{L}\mathcal{L}} + m_4^2 |V_R\rangle_{\mathcal{S}\mathcal{L}} |V_S\rangle_{\mathcal{L}\mathcal{S}}) |V\rangle].
\end{aligned} \tag{5.8}$$

We can not distinguish photons which pass through $\mathcal{L}\mathcal{S}$ and $\mathcal{S}\mathcal{L}$. These photons are extracted and other photons which pass through $\mathcal{L}\mathcal{L}$ and $\mathcal{S}\mathcal{S}$ are discarded, which can be distinguished by checking the arrival time of the photons. Then we postselect

$$\begin{aligned}
& \frac{1}{2} [m_1^2 |H_R\rangle_{\mathcal{L}\mathcal{S}} |H_S\rangle_{\mathcal{S}\mathcal{L}} |H\rangle + m_1 m_4 (|H_R\rangle_{\mathcal{L}\mathcal{S}} |V_S\rangle_{\mathcal{L}\mathcal{S}} |V\rangle \\
& + |V_R\rangle_{\mathcal{S}\mathcal{L}} |H_S\rangle_{\mathcal{S}\mathcal{L}} |H\rangle) + m_4^2 |V_R\rangle_{\mathcal{S}\mathcal{L}} |V_S\rangle_{\mathcal{L}\mathcal{S}} |H\rangle].
\end{aligned} \tag{5.9}$$

As you can see, $\frac{1}{2} m_1 m_4 (|H_R\rangle_{\mathcal{L}\mathcal{S}} |V_S\rangle_{\mathcal{L}\mathcal{S}} |V\rangle + |V_R\rangle_{\mathcal{S}\mathcal{L}} |H_S\rangle_{\mathcal{S}\mathcal{L}} |H\rangle)$ is invariant under the collective channel noise. Performing the parity checking and decoding, they can successfully share $|\phi^+\rangle$.

We now discuss the success event. The trajectories of the photons of success event is shown in Fig. 5.4. The red lines are the trajectories of the signal photon and the blue lines are that of the

ancillary photon. $|H_S\rangle$ photon and $|H_R\rangle$ photon pass through the same route, while $|V_S\rangle$ photon and $|V_R\rangle$ photon also pass through the same route. An important point is that, in this case, H polarized photon and V polarized photon experience the same channel noise, respectively, regardless of the different propagation direction, i.e., $|H_S\rangle \rightarrow m_1|H_S\rangle$, $|H_R\rangle \rightarrow m_1|H_R\rangle$ and $|V_S\rangle \rightarrow m_4|V_S\rangle$, $|V_R\rangle \rightarrow m_4|V_R\rangle$, respectively. The specific feature of entangled state is that a disturbance on one half of the photon pair is equivalent to a similar disturbance on the other half of the photon pair. Thus we can regard $m_1|H_S\rangle$ as $m_1|H_A\rangle$ and $m_4|V_S\rangle$ as $m_4|V_A\rangle$, where A represents the possessor of the photon. This property makes a two-qubit DFS scheme possible regardless of the counter propagation of the ancillary photon, which is essential to boost up the efficiency to be proportional to T .

5.3 Discussions

5.3.1 Discussion1- Robustness against the unbalance of the transmission efficiency

We have shown the robustness against the channel noise in a quantitative way. This includes the unbalance of the transmission efficiency of the two channels. We here discuss the robustness against the different transmission efficiency of the two channels in a qualitative way.

Suppose that the transmission efficiency of the channel $\bar{1}$ ($\bar{2}$) is η_1 (η_2). In order to understand qualitatively, let us reconsider the trajectory of the two photons of the success event. In this case, as shown in Fig. 5.5, H polarized photon experience η_1 , while V polarized photon experience η_2 . In the success event, the state is a superposition state of $|H_R V_S\rangle$ and $|V_R H_S\rangle$. This means that if the signal photon pass through the channel $\bar{1}$, the ancillary photon pass through the channel $\bar{2}$. On the other hand, if the signal photon pass through the channel $\bar{2}$, the ancillary photon pass through the channel $\bar{1}$. In both cases, one photon experience η_1 and the other photon η_2 , and the net effect is $\eta_1 \eta_2$. Thus the unbalance of the transmission efficiency of the two channel dose not affect the fidelity of the state.

5.3.2 Discussion2- Interpretation

As discussed in Chapter 3, a four-qubit DFS is robust under a general collective noise, however, in general, a two-qubit DFS protocol is not robust against a general noise. We now consider why our protocol is robust against a general type of the channel noise, in spite of a two-qubit DFS scheme.

As discussed above, the signal photon is protected from the phase noise by DFS. An important feature is that the proposed protocol is designed to eliminate the state which is affected by the polarization rotation by splitting the communication channel into two transmission lines using PBSs.

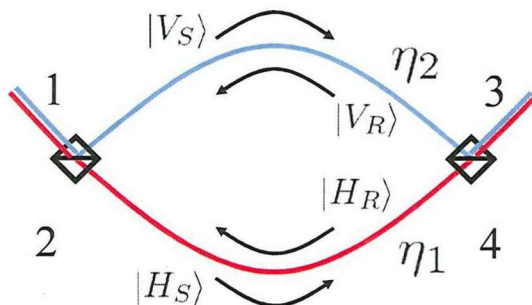


Figure 5.5: The trajectory of the signal photon and the ancillary photon. The red (blue) line represents the trajectory of the H (V) polarized photon. η_1 and η_2 represent the transmission coefficient of the channel $\bar{1}$ and channel $\bar{2}$, respectively.

In other words, if the signal photon and the ancillary photon are affected by the polarization rotation noise, photons appear at port 2 (ancillary photon) or port 4 (signal photon), and they are discarded by the postselection. By extracting only unaffected state, at the cost of the success probability, they can share entangled state against a general channel noise.

The alternative protocol that achieves both the robustness and high efficiency is proposed. The scheme is implemented using the polarization and the time-bin. In this case, the signal photon is protected from the phase noise using DFS, which is the same strategy as the above protocol. Instead of using two transmission lines, the time-bin is used to postselect the state which is not affected by the polarization rotation. Postselecting the event where both the signal photon and the ancillary photon pass through LS or SL paths ensures that these photons have not been affected by polarization rotation. Arrival time of the photons tells Alice and Bob that the photons have passed the $\mathcal{L}\mathcal{L}$ or $\mathcal{S}\mathcal{S}$, which indicates that photons are affected by the polarization rotation. An important point is that both schemes protect the signal photon by DFS and extract the state which is not subjected to the polarization rotation. Thus proposed schemes achieve the same robustness.

5.3.3 Discussion3-Application range of our protocol

We have shown the robustness and the high efficiency of the proposed protocol. In this section, we discuss the application range of the proposed protocol.

We have shown that the protocol is applicable to the channel such as optical fibers. We now

consider the case where the channels are composed of non-reciprocal media¹. For such media, the matrix for the forward propagation² is written as

$$M' = \begin{pmatrix} m'_1 & m'_2 \\ m'_3 & m'_{1*} \end{pmatrix}, \quad (5.10)$$

and the matrix for backward propagation is written as

$$\overleftarrow{M}' = \begin{pmatrix} \bar{m}'_1 & \bar{m}'_2 \\ \bar{m}'_3 & \bar{m}'_{1*} \end{pmatrix}. \quad (5.11)$$

Unlike the channel with only reciprocal media, the relation (2.17) does not hold. Let us evaluate the total state after transmitting photons. As usual, Alice prepare the $|\phi^+\rangle$ as an initial state and Bob prepares $|D\rangle$ polarization state. Let the transformation matrices of the channel $\bar{1}$ be

$$M' = \begin{pmatrix} m'_1 & m'_2 \\ m'_3 & m'_{1*} \end{pmatrix}, \quad \overleftarrow{M}' = \begin{pmatrix} \bar{m}'_1 & \bar{m}'_2 \\ \bar{m}'_3 & \bar{m}'_{1*} \end{pmatrix}, \quad (5.12)$$

and of the channel $\bar{2}$ be

$$L' = \begin{pmatrix} l'_1 & l'_2 \\ l'_3 & l'_{1*} \end{pmatrix}, \quad \overleftarrow{L}' = \begin{pmatrix} \bar{l}'_1 & \bar{l}'_2 \\ \bar{l}'_3 & \bar{l}'_{1*} \end{pmatrix}, \quad (5.13)$$

respectively. After the photons pass through the channel $\bar{1}$ and $\bar{2}$, signal photon is transformed as $|H_S\rangle \rightarrow m'_1|H_S\rangle + m'_3|V_S\rangle$ and $|V_S\rangle \rightarrow l'_2|H_S\rangle + l'_{1*}|V_S\rangle$, while the ancillary photon is transformed as $|H_R\rangle \rightarrow \bar{m}'_1|H_R\rangle + \bar{m}'_3|V_R\rangle$ and $|V_R\rangle \rightarrow \bar{l}'_2|H_R\rangle + \bar{l}'_{1*}|V_R\rangle$. The state after photons pass through the PBSs becomes

$$\begin{aligned} & \frac{1}{2} [(\bar{m}'_1 m'_1 |H_R H_S\rangle_{13} + \bar{m}'_1 m'_3 |H_R V_S\rangle_{14} + \bar{m}'_3 m'_1 |V_R H_S\rangle_{23} + \bar{m}'_3 m'_3 |V_R V_S\rangle_{24}) |H_A\rangle \\ & + (\bar{m}'_1 l'_2 |H_R H_S\rangle_{14} + \bar{m}'_1 l'_{1*} |H_R V_S\rangle_{13} + \bar{m}'_3 l'_2 |V_R H_S\rangle_{24} + \bar{m}'_3 l'_{1*} |V_R V_S\rangle_{23}) |V_A\rangle \\ & + (\bar{l}'_2 m'_1 |H_R H_S\rangle_{23} + \bar{l}'_2 m'_3 |H_R V_S\rangle_{24} + \bar{l}'_{1*} m'_1 |V_R H_S\rangle_{13} + \bar{l}'_{1*} m'_3 |V_R V_S\rangle_{14}) |H_A\rangle \\ & + (\bar{l}'_2 l'_2 |H_R H_S\rangle_{24} + \bar{l}'_2 l'_{1*} |H_R V_S\rangle_{23} + \bar{l}'_{1*} l'_2 |V_R H_S\rangle_{14} + \bar{l}'_{1*} l'_{1*} |V_R V_S\rangle_{13}) |V_A\rangle]. \end{aligned} \quad (5.14)$$

As you can see, which state we postselect, we can not extract the state that is not affected by the channel noise. Thus the proposed protocol is not applicable to the channels which is composed of the nonreciprocal media.

This can be interpreted as follows: In Sec. 5.1, the matrices for the forward propagation are described by (5.2) and the backward propagation by (5.3). Compared these matrices, we aware that

¹The channel that the relation (2.73) does not hold.

²In general case, we should have $M' = \begin{pmatrix} m'_1 & m'_2 \\ m'_3 & m'_4 \end{pmatrix}$ in stead of (5.10).

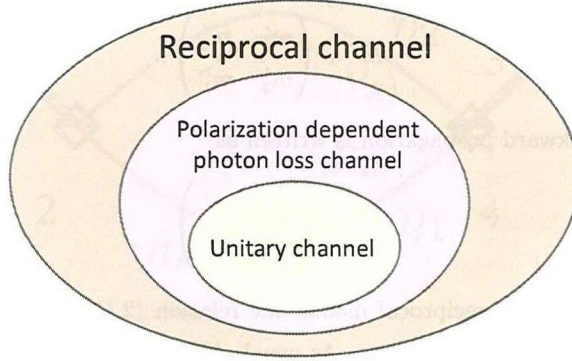


Figure 5.6: The application range of the proposed protocol. Our protocol works against the all the channels which are made of the reciprocal media.

the matrix elements of the forward propagation M_{11} and M_{22} are the same as that of the backward propagation \overleftarrow{M}_{11} and \overleftarrow{M}_{22} , respectively. Extracting only the success event, i.e., the signal photon and the ancillary photon appear at port 1 and 3, the signal photon becomes $|H_S\rangle \rightarrow m_1|H_S\rangle$ and $|V_S\rangle \rightarrow m_4|H_S\rangle$, while the ancillary photon becomes $|H_R\rangle \rightarrow m_1|H_R\rangle$ and $|V_R\rangle \rightarrow m_4|V_R\rangle$. In other words, in case of success, the signal photon and the ancillary photon experience the same noise—noises for these photons are *symmetric*. On the other hand, comparing (5.10) and (5.11), we aware that the matrix elements of the forward propagation M'_{11} is different from that of the backward propagation \overleftarrow{M}'_{11} . Likewise M'_{22} is different from \overleftarrow{M}'_{22} . That is to say that the signal photon and the ancillary photon experience the different noise—noises for these photons are *asymmetry*. These are why we can apply the proposed scheme to the reciprocal media but can not apply to non-reciprocal media.

Can't we apply our protocol to all of non-reciprocal media? Let us consider a special case of nonreciprocal media, where the media which causes only Faraday rotation. In this case, the matrix for the forward propagation with respect to the channel $\bar{1}$ is described using rotation matrix as

$$R(\theta) = \begin{pmatrix} \cos \theta & \sin \theta \\ -\sin \theta & \cos \theta \end{pmatrix}, \quad (5.15)$$

while the backward propagation is described as

$$\overleftarrow{R}(\theta) = \begin{pmatrix} \cos \theta & -\sin \theta \\ \sin \theta & \cos \theta \end{pmatrix}. \quad (5.16)$$

As same as the channel $\bar{1}$, the matrix for the channel $\bar{2}$ is written as $R(\theta')$ and $\overleftarrow{R}(\theta')$. Postselecting the state where photons arrive at the port 1 and 3, we have

$$\frac{1}{\sqrt{2}}(\cos \theta \cos \theta' |H_R V_S\rangle_{13} + |V_R H_S\rangle_{13}). \quad (5.17)$$

In a similar way, postselecting the photons at the port 2 and 4, we obtain

$$\frac{1}{\sqrt{2}}(\sin \theta \sin \theta' |H_R V_S\rangle_{24} + |V_R H_S\rangle_{24}). \quad (5.18)$$

Thus, even if the channels are made of nonreciprocal media, there are case where we can share an entangled state faithfully.

5.4 Summary

In conclusion, we have proposed an extended protocol based on DFS that achieves both the robustness and the efficiency simultaneously. Our protocol is robust against not only phase noise of the channel, but also a general (phase noise + polarization rotation) type of the channel noise. This scheme is not only robust one but also efficient one that achieve the success probability to be proportional to T . This can be realized by using counter-propagating weak coherent light pulse as an ancillary photon instead of the single photon, whose idea is proposed by Ikuta *et al.* The robustness of against such a noise is also realized using alternative method—the time-bin. The setup of the two schemes are different, however, the fundamental idea of these schemes are the same, i.e., both of the schemes, qubits are protected from phase noise using DFS, while polarization state which is affected by the polarization rotation is eliminated by the postselections. At the end of this chapter, we have discussed the application range of the proposed protocol. Our protocol is applicable to the channels that satisfies the reciprocal relation (2.17). The inclusion relation is shown in Fig. 5.6. Our schemes provide a efficient and faithful entanglement distribution which is strongly desired in quantum information processing.

Chapter 6

Conclusion

In this thesis, we have proposed an entanglement distribution protocol which realizes a robust and efficient quantum communication. The efficiency of our protocol is proportional to the transmittance T in spite of employing the multiple qubits. This is realized by using a weak coherent light pulse with the intensity to be proportional to T^{-1} , and sending it from the receiver's side to the sender's side. Using the important property that the noise on the signal, which forms an entangled photon pair with Alice's photon, is treated as the noise on Alice's photon, we see that both the ancillary photon and Alice's photon are experienced the channel noise. This makes possible to use DFS in spite of the counter propagation of the ancillary photon. In addition, for a better understanding of the counter-propagating photons, we have introduced two coordinate systems depending on the propagating directions of the photons. Owing to this we can easily calculate the polarization-state transformation in the transmission channel.

Our protocol is a robust one which is immune to not only a collective phase noise but also a general type of the channel noise. Our protocol is based on a DFS scheme that is robust against the collective phase noise. It is known that a four-qubit scheme, which is serious with respect to the efficiency, is immune to a general noise. Our scheme is based on a two-qubit DFS, however, this protocol is immune to a general noise. This can be realized by preparing an additional transmission line in the channel and the postselection. The states which are affected by the polarization rotations are rejected by the postselection and we extract an only state which is not unaffected by the noise. We showed that this scheme is also achieved using the time-bin. The fundamental idea for the time-bin scheme is the same as that of the former scheme. Using the time-delay at sender's and receiver's side, and postselecting the photon which arrives the correct time, they can extract the state which is not influenced by the polarization rotation.

The proposed entanglement distribution protocol works under the channel with polarization

dependent photon losses. The advantage of our scheme is that it can be realized using only linear optical devices and photon detectors, which are feasible in the current technologies. In addition, the treatment of the counter propagation had already established [46], so we believe that the proposed scheme is possible to demonstrate. We expect the realization of this entanglement distribution scheme. We hope that this work become the first step to construct of the quantum communication networks that would realized in the future.

Appendix A

Appendix for Chap. 2

A.1 Bell states

$$\begin{aligned} |D\rangle &= \frac{1}{\sqrt{2}}(|H\rangle + |V\rangle), & |\bar{D}\rangle &= \frac{1}{\sqrt{2}}(|H\rangle - |V\rangle) \\ |R\rangle &= \frac{1}{\sqrt{2}}(|H\rangle + i|V\rangle), & |L\rangle &= \frac{1}{\sqrt{2}}(|H\rangle - i|V\rangle) \end{aligned}$$

$$\begin{aligned} |\psi^-\rangle &= \frac{1}{\sqrt{2}}(|HV\rangle - |VH\rangle) = \frac{1}{\sqrt{2}}(-|D\bar{D}\rangle + |\bar{D}D\rangle) = \frac{i}{\sqrt{2}}(|RL\rangle - |LR\rangle) \\ |\psi^+\rangle &= \frac{1}{\sqrt{2}}(|HV\rangle + |VH\rangle) = \frac{1}{\sqrt{2}}(|DD\rangle - |\bar{D}\bar{D}\rangle) = -\frac{i}{\sqrt{2}}(|RR\rangle - |LL\rangle) \\ |\phi^-\rangle &= \frac{1}{\sqrt{2}}(|HH\rangle - |VV\rangle) = \frac{1}{\sqrt{2}}(|D\bar{D}\rangle + |\bar{D}D\rangle) = \frac{1}{\sqrt{2}}(|RR\rangle + |LL\rangle) \\ |\psi^+\rangle &= \frac{1}{\sqrt{2}}(|HH\rangle + |VV\rangle) = \frac{1}{\sqrt{2}}(|DD\rangle + |\bar{D}\bar{D}\rangle) = \frac{1}{\sqrt{2}}(|RL\rangle + |LR\rangle) \end{aligned}$$

(A.1)

A.2 The expression of Eq. (2.17) with arbitrary coordinate systems

We have discussed the expression of the optical fiber for backward propagating photon with fixed coordinate systems as shown Fig.2.1. Here we extend to more general case where the angle between y and y' is arbitrary.

Consider the case where Alice's y axis and Bob's y axis make θ' . To do this, we introduce a new rotation matrix \tilde{T} . The y axis is fixed and the y' axis is rotated by θ' . The matrix for backward propagation is changed to

$$\begin{aligned}\overleftarrow{U}_1 &= \tilde{T}(\theta')R(\theta)W_0R(-\theta)\tilde{T}(-\theta') \\ &= \tilde{T}(\theta')ZU_1^TZ\tilde{T}(-\theta').\end{aligned}\tag{A.2}$$

This is a general description of the birefringent element for backward propagation and this is easily generalized to the model of the optical fiber, i.e., N birefringent elements. We can also reformulate the universal compensator using this relation. The matrix of a mirror is changed $-Z$ to $-\tilde{T}(\theta')Z$ and the expression of the Faraday mirror is written as

$$U_{FM} = R(\theta_F)(-\tilde{T}(\theta')Z)R(-\theta_F) = \tilde{T}(\theta')X.\tag{A.3}$$

Thus total effect is described as

$$\begin{aligned}U_{total} &= \overleftarrow{U}U_{FM}U \\ &= (T(\theta')XU_1^\dagger X\tilde{T}(-\theta'))\tilde{T}(\theta')XU \\ &= T(\theta')X.\end{aligned}\tag{A.4}$$

Here we have used the relation $ZU^TZ = XU^\dagger X$. The fluctuation of the optical fiber is completely canceled out and remains only the effect of a mirror.

Research activities

Publication

- Hidetoshi Kumagai, Takashi Yamamoto, Masato Koashi, Nobuyuki Imoto, "On the robustness of quantum communication based on decoherence-free subspace using counter-propagating weak coherent laser light pulse ", Submitted to Phys. Rev. A.

International conferences

1. Hidetoshi Kumagai, Takashi Yamamoto, Masato Koashi, Nobuyuki Imoto, "On the robustness of quantum communication based on decoherence-free subspace using counter-propagating weak coherent laser light "(poster), International Conference on Quantum Foundation and Technology, Dunhuang Hotel, Dunhuang, China, August 25 - 30, 2012.
2. Hidetoshi Kumagai, Takashi Yamamoto, Masato Koashi, Nobuyuki Imoto, "On the performance of quantum communication protocols based on decoherence-free subspaces "(poster), International workshop on heavy fermions TOKIMEKI 2011, SIGMA hall, Osaka University, Osaka, Japan, November 23 - 26, 2011.
3. Hidetoshi Kumagai, Takashi Yamamoto, Masato Koashi, Nobuyuki Imoto, "Analysis of Fault-Tolerant Quantum Computation Using Tree-Cluster State "(poster), International Conference on Core Research and Engineering Science of Advanced Materials, Life Science Center and Osaka University Convention Center, Osaka, Japan, May 30 - June 4, 2010.

Domestic conferences

1. Hidetoshi Kumagai, Takashi Yamamoto, Masato Koashi, and Nobuyuki Imoto, " On the robustness of quantum communication based on decoherence-free subspace using counter prop-

- agating weak laser light” (poster) 第9回AMO討論会, 理化学研究所 大河内記念ホール, 2012/6/15 - 16.
2. 熊谷英敏, 山本俊, 小芦雅斗, 井元信之, “逆伝播コヒーレント光を用いた DFS による量子通信の雑音耐性” (口頭), 日本物理学会 2012 年春季大会 24pBE-3, 関西学院大学 上ヶ原キャンパス, 2012/3/24 - 27.
 3. 熊谷英敏, 山本俊, 小芦雅斗, 井元信之, “On the robustness of quantum communication based on decoherence-free subspace using counter propagating weak coherent laser light” (poster) 量子情報処理プロジェクト全体会議 2011, 京都国際ホテル, 2011/12/13-16.
 4. 熊谷英敏, “Analysis of the quantum repeater using a quantum-dot spin in the Bell measurement” (poster) 平成 22 年度 G-COE 若手秋の学校「量子物性の解明と新機能」, 岡山県 岡山 いこいの村 2010/10/28-30.
 5. 熊谷英敏, 山本俊, 小芦雅斗, 井元信之, “ツリークラスターを用いたロストレラントな量子計算” (ポスター), 最先端研究開発支援プログラム「量子情報処理プロジェクト」 夏期研修会, 沖縄県 ホテルサンライズ知念, 2010/8/18-28.
 6. 熊谷英敏, “ツリークラスターを用いたロストレラントな量子計算” (ポスター), 平成 21 年度 G-COE 若手秋の学校「新しい量子物質・物性・機能の研究」, 滋賀県 休暇村近江八幡, 2009/9/14-16.

Bibliography

- [1] E. Schödinger, Die gegenwärtige Situation in der Quantenmechanik. *Naturwissenschaften* **23**, 807 (1935).
- [2] A. Einstein, B. Podolsky, and N. Rosen, *Phys Rev.* **47**, 777 (1935).
- [3] J. S. Bell, *Physics (Long Island City, N.Y.)* **1**, 195 (1964).
- [4] J. F. Clauser, M. A. Horne, A. Shimony, and R. A. Holt, *Phys. Rev. Lett.* **23**, 880 (1969).
- [5] A. Aspect, P. Grangier and G. Roger, *Phys. Rev.* **47**, 460 (1981).
- [6] M. A. Nielsen and I. L. Chuang, "Quantum Computation and Quantum Information", Cambridge University Press, (2000).
- [7] D. Deutsch, *Proc. R. Soc. London A* **400**, 97 (1985).
- [8] P. W. Shor, *Proc. 35nd Annual Symposium on Foundations of Computer Science (Shafi oldwasser, ed.)*, IEEE Computer Society Press, p124 (1994).
- [9] L. Grover, *Phys. Rev. Lett.* **78**, 325 (1997).
- [10] H. J. Kimble, *Nature* **453**, 1023 (2008).
- [11] M. Koashi, V. Bužek, and N. Imoto, *Phys. Rev. A* **62**, 050302(R) (2000).
- [12] W. Dür, *Phys. Rev. A* **63**, 020303(R) (2001).
- [13] T. Tashima, Ş. K. Özdemir, M. Koashi, and N. Imoto, *New, J. Phys.* **11**, 023024 (2009).
- [14] R. Ikuta, T. Tashima, T. Yamamoto, M. Koashi, and N. Imoto, *Phys. Rev. A* **83**, 012314 (2011).
- [15] D. Greenberger, M. A. Horne, A. Shimony, and A. Zeilinger, *Am. J. Phys.* **58**, 1131 (1990) .

- [16] M. Zukowski, A. Zeilinger, and H. Weinfurter, in *Fundamental Problems in Quantum Theory* vol. 755 Annals of the New York Academy of Sciences (Greenberger and Zeilinger Eds.) p.91 (1995).
- [17] H. J. Briegel, W. Dür, J. I. Cirac, and P. Zoller, *Phys. Rev. Lett.* **81**, 5932 (1998).
- [18] L. M. Duan, M. D. Lukin, J. I. Cirac, P. Zoller, *Nature*, **414**, 413 (2001).
- [19] N. Sangouard, C. Simon, H. de Riedmatten, and N. Gisin, *Rev. Mod. Phys.* **83**, 33 (2011).
- [20] P. van Loock, T. D. Ladd, K. Sanaka, F. Yamaguchi, K. Nemoto, W. J. Munro, and Y. Yamamoto, *Phys. Rev. Lett.* **96**, 240501 (2006).
- [21] L. Jiang, J. M. Taylor, K. Nemoto, W. J. Munro, R. Van Meter, and M. D. Lukin, *Phys. Rev. A.* **79**, 032325 (2009).
- [22] M. Zukowski, A. Zeilinger, M. A. Horne, and A. K. Ekert, *Phys. Rev.* **71**, 4287 (1993).
- [23] C. H. Bennett *et al.*, *Phys. Rev. Lett.* **70**, 1895 (1993).
- [24] A. K. Ekert, *Phys. Rev. Lett.* **67**, 661 (1991).
- [25] C. H. Bennett, G. Brassard, and N. D. Mermin, *Phys. Rev. Lett.* **68**, 557 (1992).
- [26] N. Gisin, G. Ribordy, W. Tittel, and H. Zbinden, *Rev. Mod. Phys.* **74**, 145 (2002).
- [27] D. Gottesman and I. L. Chuang, *Nature (London)* **420**, 390 (1999).
- [28] R. Raussendorf and H. J. Briegel, *Phys. Rev. Lett.* **86**, 5188 (2001).
- [29] D. A. Lidar and K. B. Whaley, Decoherence-free subspaces and subsystems in *Irreversible Quantum Dynamics*, Springer Lecture Notes in Physics, Vol. 622 (eds F. Benatti and R. Floreanini) 83-120 (Springer, Berlin, 2003).
- [30] P. Zanardi and M. Rasetti, *Phys. Rev. Lett.* **79**, 3306 (1997).
- [31] D. Kielpinski *et al.*, *Science* **291**, 1013 (2001).
- [32] L. Viola *et al.*, *Science* **293**, 2059 (2001).
- [33] J. E. Ollerenshaw, D. A. Lidar, and L. E. Kay, *Phys. Rev. Lett.* **91**, 217904 (2003).
- [34] M. Mohseni, J. S. Lundeen, K. J. Resch, and A. M. Steinberg, *Phys. Rev. Lett.* **91**, 187903 (2003).
- [35] C. F. Roos, M. Chwalla, K. Kim, M. Riebe, and R. Blatt, *Nature* **443**, 316 (2006).

- [36] Z. D. Walton, A. F. Abouraddy, A. V. Sergienko, B. E. A. Saleh, and M. C. Teich, *Phys. Rev. Lett.* **91**, 087901 (2003).
- [37] J.-C. Boileau, D. Gottesman, R. Laflamme, and R. W. Spekkens, *Phys. Rev. Lett.* **92**, 017901 (2004).
- [38] T. Yamamoto, J. Shimamura, Ş. K. Özdemir, M. Koashi, and N. Imoto, *Phys. Rev. Lett.* **95**, 040503 (2005).
- [39] P. G. Kwiat, A. J. Berglund, J. B. Altepeter, and A. G. White, *Science* **290**, 498 (2000).
- [40] M. Bourennane *et al.*, *Phys. Rev. Lett.* **92**, 107901 (2004).
- [41] J.-C. Boileau, R. Laflamme, M. Laforest, and C. R. Myers, *Phys. Rev. Lett.* **93**, 220501 (2004).
- [42] T.-Y. Chen *et al.*, *Phys. Rev. Lett.* **96**, 150504 (2006).
- [43] R. Prevedel *et al.*, *Phys. Rev. Lett.* **99**, 250503 (2007).
- [44] T. Yamamoto *et al.*, *New J. Phys.* **9**, 191 (2007).
- [45] T. Yamamoto, K. Hayashi, Ş. K. Özdemir, M. Koashi, and N. Imoto, *Nat. Photon.* **2**, 488 (2008).
- [46] R. Ikuta *et al.*, *Phys. Rev. Lett.* **106**, 110503 (2011).
- [47] R. C. Jones, *J. Opt. Soc. Am.* **38**, 488 (1941).
- [48] A. Yariv, *Optical Electronics in Modern Communications* (Oxford University Press, 1997).
- [49] M. Yoshida-Dierolf, *Opt. Commun.* **203**, 69 (2002).
- [50] N. C. Pistoni, *Appl. Opt.* **34**, 7870 (1995).
- [51] J. J. Sakurai, "Modern Quantum Mechanics", Addison-Wesley Publishing Company, (1994).
- [52] M. Martinelli, *Opt. Commun.* **72**, 341 (1989).
- [53] A. Muller *et al.*, *Appl. Phys. Lett.* **70**, 793 (1993).
- [54] J.-W. Pan, C. Simon, C. Brukner, and A. Zeilinger, *Nature* **410**, 1067 (2001).
- [55] T. Yamamoto, M. Koashi, and N. Imoto, *Phys. Rev. A* **64**, 012304 (2001).
- [56] T. B. Pittman, B. C. Jacobs, and J. D. Franson, *Phys. Rev. A* **64**, 062311 (2001).
- [57] J. Kempe, D. Bacon, D. A. Lidar, and K. B. Whaley, *Phys. Rev. A* **63**, 042307 (2001).

- [58] C. H. Bennett and G. Brassard, in *Proceedings of IEEE International Conference on Computers, Systems, and Signal Processing, Bangalore, India* (IEEE, New York, 1984), p. 175.
- [59] C. H. Bennett, *Phys. Rev. Lett.* **68**, 3121 (1992).

